Università degli Studi di Pisa
Facoltà di Scienze Matematiche Fisiche e Naturali
Corso di Laurea Magistrale in Fisica

In Silico model of Astrocytes-Neurons Interaction

Supervaisors:
Prof. Alberto Mazzoni
Prof. Angelo Di Garbo
Dott. Nicolò Meneghetti

Candidate:
Angelo Lasala

Academic Year 2021/2022

Abstract

Contents

Chapter 1

INTRODUCTION

1.1 Background

It is wholly accepted that neurons are the main protagonist in the functional and anatomical organization of the human brain. However, they can not accomplish complex cognitive processes without the presence of another non-neural cell type: the glial cells. Glia is physically collocated in proximity to neurons and, due to elaborate anatomical and functional branches organization, performs vital biological tasks. These include but are not exhaustive in the homeostatic regulation of extracellular ions concentrations, blood vessel-neuron interface and related feeding mechanism, immune function and modulation/regulation of signalling transmissions among neurons [1]. In particular, the latter aspect might underline that glial cells are not simple onlookers in information transmission but, beside the neurons, be a unit process ad take part actively in the encoding mechanism of external stimuli. Nevertheless, in the field of neuroscience and especially computational neuroscience, the functional role of this type of cell is only partially explored. During the last twenty years, several models composed of several coupled ordinary differential equations are developed to dynamically describe the bidirectional coupling between the synaptic and glial activity [6, 10]. Despite the chance of a detailed microscopic portrait, the macroscopic level of description still lacks an overview thereby glia are dealt with their physiological features.

The purpose of the present thesis is, following a bottom-up approach, to deeply investigate the neuron-glia interaction and try to build a bridge between the microscopic and mesoscopic levels of description. This link might shed light on a possible new mechanism of signalling transmission and explain some current incongruent results in computational neuroscience. Accordingly, the analyses lie in two interconnected steps. In the beginning, it needs to characterize all the dynamic aspects of the unit element, the so-called tripartite synapse that embeds the bidirectional coupling between neuronal (in particular synaptic) and glial activity. Then, starting with these results, extend the description to the neuron-glia network, namely an ensemble of neurons where the connections are provided by tripartite synapse. Numerical and approximation are suitable tools to accomplish these goals.

Simulations and Analysis overview

Simulation of neuron, synapses and astrocyte modeltripartite synapses

1.2 Highlights

1.3 Functional role of Glial Cells

The functional and anatomical complexity makes the human brain one of the most exciting systems in the universe. It continuously elaborates sensory stimuli from the environment, interfacing with it through several cognitive processes, and controls the internal activities of the entire body. Furthermore, it regulates high-level mechanisms such as consciousness and sensations. The study of the Central Nervous System (CNS), due to the intricate and variegated tasks accomplished by the brain, encompasses different levels of analysis, for instance, chemical, molecular, anatomical, and cognitive. Therefore it has always been an interdisciplinary subject to study.

The discovery of the neuron by Santiago Ramón y Cajal, Nobel Prize in Medicine in 1906, has put the stage for current knowledge of neural systems through the common efforts from different fields such as anatomy, biochemistry, physics as well as medicine and psychology. Typically a neurons is composed of three functional parties: dendrites, the soma, and the axon. Soma is the body of the neuron and contains the nucleus of the cell, dendrites are the extensions of the cell and carry input information to the neurons, and the axons are the branches of output communication. In neurons, as in the other cells, the ion channels collocated on the soma, but also on dendrites and axons, provide the fluxes of ions through the cell membrane and the electrical electrical potential difference across the membrane arisen from these fluxes is called the membrane potential. Nowadays it is clear neurons communicate with each other by the propagation of action potential, an abruptly increase of membrane potential due to the nonlinear integration process by the soma of external inputs. Furthermore, a widely assumed premise is that most cognitive processes emerge from the activity of ensembles of neurons, whose dynamics arise from complex interactions and connection involving single elements. The chemical synapses are the most common structure in the neural system that provide these interactions by the release of specific chemicals called neurotransmitters from the presynaptic neurons that bind with postsynaptic neurons causing either depolarization or hyperpolarization of their membrane potential.

Sophisticated processing of sensory information and, more in general, the ability to respond to external stimuli is a feature that humans share with most animals, resulting from the development of the complex neural structure. From a phylogenetic perspective, as the nervous systems changed from simple net structure (invertebrates) to condensed centralized brains (vertebrates), a new cell type could be recognized in morphological studies: *glia cells.* [2]

It is customary to credit pathologist Virchow with the discovery of glia. Following the idea that only connective tissue is capable of becoming inflamed, he found a connective tissue not only beneath the ependyma, but penetrating the mass of the brain, filling all interstices among nerve cells and their fibres, and also separating nervous tissue from blood vessels. In the collection of Virchow's papers published in 1856, there is the first use of the term neuroglia. [4]. Other illustrious researchers at the beginning of the nineteen century brought paramount contributions to the glia cause: Golgi led to the recognition of multipolar glial cells, and also their intimate relationship to blood vessels, the same

Ramón y Cajal legitimated neuroglia as the "third element" of the nervous system, and Rio-Hortega in 1920 crystallizing the still-accepted classification of glia. [3]

Interestingly, the glial cells are the main type of both neuronal and non-neuronal cells in the fully developed human brain, indeed they account for $\sim$ 90 percent of total cells. The most numerous glial cells appear to fall into three different types: oligodendrocytes, microglia and astrocytes. Despite the different origins, both cells type share a common feature, that is physical proximity to neurons by an elaborated breaches anatomy that interweaves with neuronal processes, which allows performing several biological tasks. Oligodendrocytes, for example, are responsible for the myelination of axons, which is essential to support the signal transmission over long distances (Nave 2010, NG perspective) otherwise, microglia are responsible for immune function including the mechanism of neural protection.

Astrocytes, literally star-like cells, are the most numerous and diverse glial cells in the CNS. There is a common agreement regarding their crucial roles in controlling the homeostasis of surrounding neurons, with a fundamental role in energy metabolite supply and neurons-vascular interface [5]. One of the first possible recognized functions of astrocytes is their importance in the maintenance of extracellular K^+ concentration, electrophysiological recordings in vivo, indeed, implicate modulation of K^+ by astrocytes in the regional controls of neural excitability in the healthy brain. The resting membrane potential of neurons depends on intra- and extracellular concentrations of different ions, thus changes in extracellular K^+ concentration can alter neuronal excitabilit.

This is only one possible pathway where astrocytes could have an active role in the signalling transmission, indeed, besides these homeostatic functions, astrocytes display dynamic signalling with neurons and synapses. For a cell to be considered an active element in the brain coding network, it should be able to: (i) receive incoming information; (ii) integrate and code that information; and (iii) transfer the information to other cells. Neurons have the ability to performs these actions due to their anatomical characteristics and intrinsic electrical properties. Because glial cells are notorious electrically passive, their code must rely on mechanisms different from membrane potential.

Despite the lack of electrical features, they show intricate cellular excitability originating from membrane receptors in the cytosol, this is the case of second messengers like inositol 1,4,5-trisphosphate (IP_3) and intracellular calcium. In these regards, they fulfil the three requirements by a glia code based on second messenger oscillations. Among these, calcium signalling is the most studied one, arguably because of the availability of indicators to monitor intracellular calcium as well as for its recognized function as an intracellular messenger in a multitude of other cells (Berridge et all, 2000, a NG perspective).

Astrocytes, therefore, can sense the synaptic activity induced by several neurotransmitters such as glutammate, GABA, acetylcholine and ATP, that trigger intracellular processes causing variation in Ca^{2+} concentration. Decoding these signals is a necessary step for any mechanism that uses this code to perform a downstream action. In this sense, the ability to release neuroactive molecules, called gliotransmitters, when calcium overcomes a threshold value makes the astrocytes able to influence neuronal activity and synaptic transmission. This feature takes the name of *gliotransmission* and bears the widest implication in information processing.

All these features can be regarded as evidence of the purpose of glia for being an integral part of both structure and function of neural networks. The recognition that glia cells could be much more than passive elements has therefore been accepted as a revolution of the classical Neuron paradigm of the brain in favor of a more comprehensive Neuron-Glia paradigm (cit Heydon 2001, ch1). There is no other concept that epitomizes the Neuron-Glia paradigm better than the tripartite synapses, whereby the astrocyte is the third active element in synaptic information transfer besides the pre- and postsynaptic, sensing synaptically-released neurotransmitters by a variety of mechanisms, and signalling back to synaptic by gliotransmission.

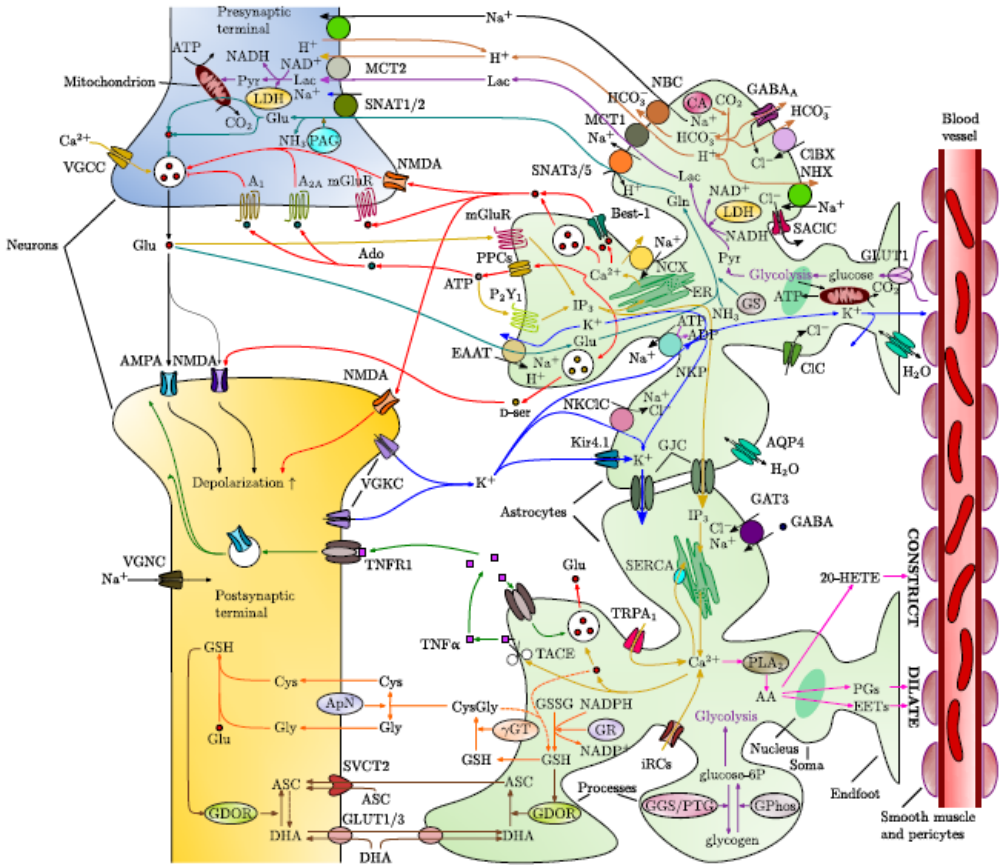

Figure 1.1: **Common interaction between astrocytes and glutammatergic synapes**. Simplified illustration of the main pathways of interaction of astrocytes with neurons at glutammatergic synapses, whereby the intimate and intricate relation between the two elements is clearly visible. Taken from De Pittà (2020) [2].

Since their discovery, astrocytes have been the subject of growing interest, nonetheless, their active role in the framework of neuronal network theory has only been partially explored. Neglecting the glia pathway of interaction might leads to a warped description of the functional brain physiology because the modulation of neural excitability and synaptic transmission by glia could regulate network activity dramatically.

The important role of theoretical and computational modelling lies in this framework. In the field of neuroscience, instead, it is not always possible to record all the measurements needed to understand a study case and the difficulty in brain activity measurements and

recordings in vivo leads to adopting both mathematical and computational approaches to overcome experimental issues. One of the central tasks of computational neuroscience is to bridge different levels of description, i.e. from a single ions channel to an entire neural network, by simulation and mathematical theory. The link can be built in two different directions, from microscopic to macroscopic scales (bottom-up) or from behavioural target functions to properties of components (top-down) [16].

During the years, the joint effort of theoretical neuroscientists has led to improving the computational modelling of neural network to the point of simulating well-recorded network activities such as asynchronous irregular firing or oscillatory firing [20, 21, 22]. We want to stress that this is not a mere theoretical challenge since, reproducing real physical phenomena through equations, approximations and simplifications mean fully understanding the systems and extrapolating among all possible mechanisms only that drive the dynamics.

In the content of the neuron-glia network, there are only a few available models that different from each other by network configuration and different choices of the astrocytic signalling pathway. For instance, the model by Ullah [24] considers the homeostasis regulation of extracellular K^+ and Na^+, while Stavachennko et al consider the effect of gliotransmission by glutammatergic synapses. Interesting, in the latter case, the author dealt with a neural network based on the well-tested hippocampal basket and found that the depression of synapses within an astrocytic domain correlates with a decrease in neuronal firing and synchronization [25]. However, they mimicked the astrocytic modulation study, namely did not consider a theoretically plausible feedback effect associating neuronal firing frequency with astroglial actions.

In this regard, the present thesis aims to follow a bottom-up approach to filling the gap between microscopic and macroscopic aspects of neuron-glia interaction and underline the possible dynamical changes that arise both at the synaptic and network level.

From the point of view of Physics, neurons, synapses and astrocytes are nonlinear dynamical systems that intricately interact with each other, whereby we follow the framework of Dynamical Systems Theory to shed light on interacting pathways of tripartite synapse and signalling transmission. In particular, the theory of bifurcation and, more in general, the qualitative description of complex system dynamics are the theoretical tools able us to explain the effect of gliomodulation.

Thereafter, we develop a spiking network model in order to explain the possible implication of the presence of glia in the network dynamics. At this level of detail, it is possible to build a structured network of hundreds or thousands of elements coupled together in different fashions. Most importantly, in this way, we can tack into account the dynamics of every element, thereby maintaining a well-detailed description of microscopic processes and simultaneously portraying the important macroscopic phenomena.

In the following paragraphs, we describe in detail the theoretical tools in nonlinear dynamical theory and underline the limits and constraints of this procedure when it is applied to complex biological systems. Then we introduce the framework of neural networks, namely interacting neurons, to elucidate how collective phenomena could arise and monitor by macroscopic observables.

1.4 Brain Cells as Dynamical Systems

The world is an ensemble of systems that evolve in time and interact with each other. Although the study of these dynamical systems is now a multidisciplinary subject, physics has built over the century the right mathematical setting to deal with them. The study of the gravitational two-body problem by Newton in the middle of 1600 through ordinary differential equations (ODEs) gave rise to the theory of dynamical systems. Despite the possibility of reaching an analytical solution for this system, the extension of the three-body problem turned out to be essentially impossible to solve.

The breakthrough came with the work of Poincaré in the late 1800s [26] where he introduced a new method based on qualitative rather than quantitative descriptions to deal with the celestial motion. Poicaré's powerful approach is completely general and can be applied also to complex nonlinear dynamical systems, like biological ones. This was a turning point because, in contrast to linear systems, nonlinear ones cannot be separated into different parts, and the principle of superposition fails spectacularly.

In general, dynamical systems could be described by an ODE of this form [1]:

$$\frac{d\mathbf{x}}{dt} = f(\mathbf{x}, t, \boldsymbol{\mu}) \tag{1.1}$$

with $\mathbf{x} \in U \subset \mathbb{R}^n$, $t \in \mathbb{R}^1$, and $\boldsymbol{\mu} \in W \subset \mathbb{R}^p$ where U and W are respectively open set in $\mathbb{R}^n$ and $\mathbb{R}^p$. The vector $\mathbf{x}$ represents the state of the system, and the space of dependent variables in $\mathbb{R}^n$ is the *phase space*. Typically, the vector $\boldsymbol{\mu}$ stands for the ensemble of *parameters* that characterize the systems, whereas the independent variable t is often referred to as *time*. In contrast to nonautonomous ordinary differential equation (1.1), *autonomous* or time independent ODEs do not explicitly depend on time, i.e. the vector filed f read as $f(\mathbf{x}, \boldsymbol{\mu})$.

In the field of neuroscience, most model concerns voltage and second messenger to understand the cell's intrinsic properties. Due to their electrical features, neurons are typically modeled using an equivalent electric circuit. The membrane is made by a lipid bilayer that acts as a passive capacitor C_m. Ionic channels creating ionic currents acts as dynamical resistances R and the resting potential membrane E_l is represent by a voltage source. This is the setting for Hodging and Haxley's pioneering work in modelling neuronal excitability. They developed a remarkable and detailed biophysical model in 1952 [34] of membran potential dynamics that is still widely used nowadays. They discovered that the principal membrane ionic currents were due to sodium and potassium diffusion and built their model by 4 differential equations:

$$\begin{aligned}
C_m \frac{dV}{dt} &= -[\bar{g}_{N_a} m^3 h(v - E_{N_a}) + \bar{g}_K m^4 (V - E_K) + \bar{g}_l (V - E_l)] \\
\tau_m \frac{dm}{dt} &= m_\infty(V) - m \\
\tau_h \frac{dh}{dt} &= h_\infty(V) - h \\
\tau_n \frac{dn}{dt} &= n_\infty(V) - n
\end{aligned} \tag{1.2}$$

[1] Here we briefly summarize the main aspect of dynamical systems present in this thesis, for detailed and rigorous treatment we refer to [27, 30, 28]

this model embeds psychological features and reproduces experimental data about action potential generation of giant squid's axon. On the other hand astrocytes, the main type of glial cells in the brain, do not generate action potentials as neurons do, yet they can transfer information to other cells and encode information in response to external stimuli by employing "excitable"-like rich second messengers dynamics. Many model of a general chimical A, are based on the interpretation of essential fluxes and described using the language of differential equations. The rate of change of $[A]$ in the cytosol, $A(t)$, depends on a combination of fluxes contributing positively (J_{in}) and negatively (J_{out}):

$$\frac{dA}{dt} = J_{in} + J_{out} \tag{1.3}$$

where the fluxes depends on the open-close mechanism of endoplasmatic receptors regulates the concentration of second messengers in astrocytic cytosol.

Give a set of (1.1), a solution $\mathbf{x}(t)$ of (1.1), from some interval $I \subset \mathbb{R}^n$, is a function from I to $\mathbb{R}^n$ such that $\mathbf{x}(t)$ satisfies (1.1):

$$\frac{d\mathbf{x}(t)}{dt} = f(\mathbf{x}(t), t, \boldsymbol{\mu}) \tag{1.4}$$

Abstractly, the goal will be to understand the geometry of solution curves in phase space. Therefore, following the qualitative approach introduced by Poincaré, we will not be interested in the exact solution of equation (1.4). The general approach starts to individuate the *steady states* (or fixed points), namely the solutions that do not change in time ($f(\mathbf{x}, \boldsymbol{\mu}) = 0$). Once we find these peculiar states, it is natural to try to determine the nature of their stability. Roughly speaking, a steady state $\bar{\mathbf{x}}$ is *stable* if solutions close to $\bar{\mathbf{x}}$ at a given time remain close to $\bar{\mathbf{x}}$ for all later time, otherwise, if the neighbour trajectories run far away from $\bar{\mathbf{x}}$ the fixed point is *unstable*. One of the most fascinating aspects of autonomous and nonlinear systems is the behaviour close to the steady states: stable or unstable, periodic or aperiodic, and even chaotic orbits could arise in the phase space depending on the mathematical features of the vector field, like the stability, and the choice of parameters.

1.4.1 Bifurcation Theory

The natural question we ask is how the stability or instability is affected as μ is varied, in other words, what is the sort of the dynamics concerning the variations of one or more parameters. The theorem of bifurcation of fixed points gives us an important clue about the answer. In the textbook by Wiggings [28] is present a definition for the one-dimensional and one-parameter family vector field:

Bifurcation of fixed points: consider one-dimensional autonomous vector field

$$\frac{dx}{dt} = f(x, \mu) \tag{1.5}$$

where f is a $\mathbf{C}^r$ [2] function on some open set in $\mathbb{R}^1 \times \mathbb{R}^1$. A fixed point of one-parameters $(\bar{x}, \bar{\mu}) = (0, 0)$ is said to undergo a *bifurcation* at $\bar{\mu}$ if the flow for μ near 0 and x near 0 is *not* qualitative the same as the flow near $(\bar{x}, \bar{\mu}) = (0, 0)$.

[2] Usually $\mathbf{C}^5$ will be sufficient

This definition is not more general: the vector field must have a precise smooth conditions, the fixed point lies in the origin of phase space, and the phrase "qualitative the same" is only adequate for the study of the bifurcation of one-dimensional dynamical systems [3]. Nevertheless, Meiss in his book [29] gives an alternative definition:

Bifurcation: A bifurcations is a *qualitative* change in dynamics occurring upon a small change in a parameter.

According to the approach described by Poincaré, both the definition emphasize the role of qualitative dynamical changes, however, the second puts the bifurcation into a wide sense framework: it is an extremely general theory that stands for the ensemble of techniques to qualitative understand how the control parameter drives the dynamics.

However, knowing physiologically proprieties does not suffice to determine what the cell is doing and why it is doing it. Both neurons and glial cells, indeed, can exhibit different responses in terms of their code by varying one or more characteristics of their inner proprieties. Neurons, for example, can exhibit completely different spiking activity to the same injecting current [35], whereas astrocytes respond with amplitude or frequency modulation to periastrocytic neurotransmitter concentration [13]. In this regard bifurcation is the most suitable tool for a systematic study of the relationship between physiology and the computational properties of brain cells. Izhikevich, in the preface of his book, brilliantly summarized the above considerations with the following sentence:

"Information-processing depends not only on the electrophysiological properties of neurons but also on their *dynamical properties*. Even if two neurons in the same region of the nervous system possess similar electrophysiological features, they may respond to the same synaptic input in very different manners because of each cell's bifurcation dynamics."

Izhikevich, preface of *Dynamical Systems in Neuroscience: The Geometry of Excitability and Bursting* [30]

1.4.2 Noisy Systems and Mean Field Description

Unfortunately, in the real world, most (if not all) physical phenomena can not be described by a set of deterministic ODEs like 1.1, most of the time indeed, the noise sources can not be neglected for a faithful description of reality. Several noise sources affect all aspects of nervous system function and neuron activity at different time and space scales, from the open-closed mechanism of ion channels to the signalling transmission over long distances as illustrated in Figure (1.2).

[3] The phrase "qualitative the same" is a bit vague and it can be made precise only in the context of one-dimensional vector field by substituting the term $\mathbf{C}^0$-equivalent.

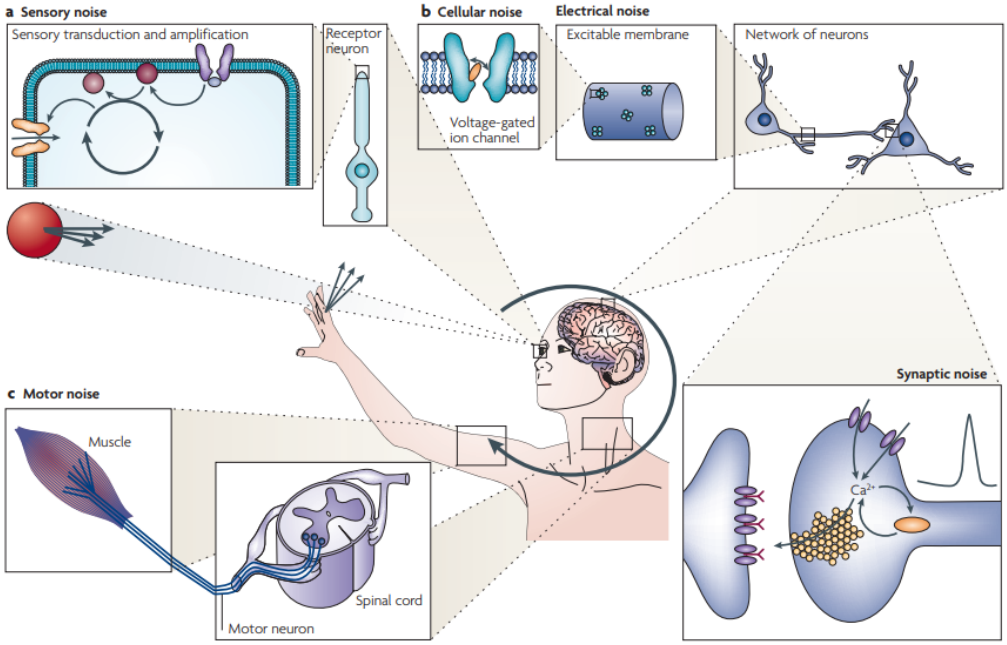

Figure 1.2: **Overview of the behavioural loop and the stages at which noise is present in the nervous system**. How noise permeates every level of the nervous system, from the perception of sensory signals to the generation of motor responses, and poses a fundamental problem for information processing. Taken from Faisal (2008) [39].

Accordingly, the recording of some measurable quantities, such as spike timing and membrane potential, show a cert level of *variability*, in particular, analysis of physiological data suggests that both neurons and astrocytes in vivo fire irregularly [40, 41]. Trial-to-trial variability can arise from two distinct sources. We have already mentioned the deterministic variability of neuron activity due to dynamical proprieties. The other type of variability is strictly related to the noise: the spikes trains of a single neuron vary from one trial to the other by repeating an experiment several times, namely when external stimuli, such as the sensory input or task goal, are kept as equal as possible across different trials. To take into account the latter kind of variability the deterministic description is not enough and we explicitly need to consider a noise term in the system's equation:

$$\frac{d\mathbf{x}}{dt} = f(\mathbf{x}, t, \boldsymbol{\mu}) + \text{noise source} \tag{1.6}$$

Equation (1.6) represents a stochastic differential equation (SDE) with additive noise term [4]. The most important consequence is that by fixing the parameters space $\boldsymbol{\mu}$ (therefore the vector field f) and the initial condition $\mathbf{x}_0$, the time course of variables $\mathbf{x}$ is different over several realizations, hence the system examines a widespread region of accessible phase space. From the experimental and computational point of view, the goal is to record an ensemble of data about the same system with identical initial conditions and parameter space, and then estimate the dispersion of the dynamical variables around their mean values. Accordingly, with a large data set, it is possible to have a robust portrait of underpinning deterministic rules driving the variables' time evolution, and the dispersion effect induced by noise terms.

[4]The world of SDE is a minefield. Here we consider only the most general noise term to treat trial-to-trial variability in neurons model. However, more complex situations like multiplicative noise might be present.

Another typical approach is the mean field approximation, a general analytic method that returns the dynamics of mean quantities. Starting from the analytic approximation, we can understand which of all parameters drive the variable time evolution and extrapolate, among all the possible underpinning mechanisms, only the most influential ones. The reasoning of the mean field is summarized by the following steps:

1. Consider an ensemble of n_S equation (1.6) with the different realization of noise with the same statistical proprieties.
2. Compute trial averaged dynamics in terms of mean quantities $\bar{\mathbf{x}} = \frac{1}{n_S}\sum_l^{n_s} \mathbf{x}_l$
3. Write down the ODEs for mean quantities $\bar{\mathbf{x}}$ using the statistical proprieties of noise.

The above computational and analytical approaches share the effort to "clear" the results to stochasticity, thus we expect that the former are in good agreement with the latter ones. More precisely, all the mathematical approximations and hypotheses (if correct) have to bring a solution as close as possible to the real-world data, i.e. computational one, otherwise, these assumptions can not be considered correct and must be changed.

In conclusion, the bifurcation intented as the qualitative study concerning the small variation of a control parameter and the numerical/analytical mean field description are two powerful tools to shed light on the dynamical features of a system. Importantly, these tools are not mutually exclusive. Indeed, how the mean quantities are affected by a small variation of a control parameter is a legitimate question in the field of random motions, and the answer lies in the wide sense bifurcation framework.

1.5 Spiking Neural Model

The neuron is the unit element of processing information in the nervous system however, it does not accomplish alone the multitude of elaborate cognitive functions. The brain contains millions of neurons which are organized in a hierarchical organization of connected populations. In this sense, the brain is interpreted as a complex system in which the connection of nonlinear elements brings out collective phenomena. Neural populations, indeed, show a multitude of dynamical behaviours from asynchronous to synchronous activity. The latter is elicited from the cooperative organization of neurons that show a synchronization not presented in single elements. Network oscillations are common and prominent features that are involved in cognitive and sensory processes, for example, oscillations in the γ-band (30-100 Hz) are robustly triggered by sensory stimuli in the cortex. Such cooperative many-body systems are characterized by rich phase space and high-dimensional dynamics used to continuously interact with the external environment [47]. Importantly, the behaviour of a population is deeply characterized by the dynamical model of neurons and the type of connectivity. In the general framework, let's consider a population of N neurons in which the state of a single unit evolves according to an equation of type (1.6), thus the ensemble of these states describes the time evolution of the entire population:

$$\Omega_N = \{\mathbf{x}_1, \mathbf{x}_2, ..., \mathbf{x}_N\} \tag{1.7}$$

Neuronal code is based on the propagation of action potential that marks times at which the cell membrane at the soma reaches the firing threshold. Thus, there is a sequence of action potentials containing information about the membrane potential at

the neuronal cell body, and it is the information carried by the train of action potentials that provides information at the projection targets for the neurons. This train of action potentials, the spike train, is the element of a neural code [48]. Accordingly, the activity of neurons j is a sum of point events in time

$$\rho_j(t) = \sum_k \delta(t - t_{j_k}) \tag{1.8}$$

where the Delta function $\delta(t - t_{j_k})$ stand for the spikes train of neurons j. Moreover, the variability of the neural response causes the inter-spike intervals (ISI) to have a certain distribution, therefore a statistical approach is mandatory to obtain the right picture of signalling decoding. Given a spike at time t_0, we have to find the probability to observe other one at time t_1, i.e. $P(n+1, t_1|n, t_0)$. If the events are independent then the probability distribution is well described by the Poisson distribution whereby the firing rate $\nu(t)$ is the only parameter to completely describe the statistic.

The response of a cert neurons i in the population Ω_N depends on the activity ρ_j of its linked neurons N_i

$$\frac{dx_i}{dt} = f(\mathbf{x}_i, t, \boldsymbol{\mu}_i) + \sum_{j=1}^{N_i} s(\rho_j) \tag{1.9}$$

Equation (1.9) limps all the characteristics that drive the population dynamics[5].The time evolution of variable x_i affected by the sum of the inputs is described by the choice of the model, i.e. the vector field $f(\mathbf{x}_i, t, \boldsymbol{\mu}_i)$ and the connection features that are the synaptic activity $s(\rho_j)$ and the connectivity links.

In most neural networks, the connection is provided by chemical synapses which elaborate the input spikes train from the so called presynaptic neurons to transmit to the postsynaptic one. From a biological point of view, the involved mechanisms of synaptic activity are the transduction of action potential into a release of neurotransmitters, hence we can deal with synapses as a dynamical system with finite characteristic timescales which shape the time-evolution of pulse-like action potential communication. More precisely, a simple way of describing the time course of synaptic input is as a decaying exponential:

$$s(\rho_j(t), t) = \sum_k \frac{1}{\tau_{syn}} e^{-\frac{t-t_{j_k}}{\tau_{syn}}} \Theta(t - t_{j_k}) \tag{1.10}$$

where $\Theta(t - t_{j_k})$ is the Heaviside function and therefore every exponential term is considered only starting from the spike arrivals t_{j_k} and τ_{syn} is the characteristic time constant. The demanding issues concerning the connections because of the real connectivity of different neurons in different layers is still partially unknown due to the limited experimental data. A least, some plausible estimates of connection probabilities exist, for example in some cases the connection probability is considered distance-dependent or assumes randomly within and between populations. Despite the existence of different schemes, from a computational and modelling perspective, the connectivity is represented by a matrix involving a number of rows and columns equivalent to the number of neurons in the network. In this connectivity matrix $C_{i,j}$, the link between postsynaptic neuron i and presynaptic neuron j receives a value of 1, otherwise, the matrix element is 0. In these regards, equation 1.10 becomes:

[5]We consider here only the action of inputs on a single variable x_i of the model. The variable affected by synaptic activity might for instance be either the membrane potential or the membrane capacitance.

$$\frac{dx_i}{dt} = f(\mathbf{x}_i, t, \boldsymbol{\mu}_i) + \sum_{j=1}^{N} C_{i,j}\, w_{i,j} \sum_k \delta(t - t_{j_k}) + I_{ext}(t) \tag{1.11}$$

where $w_{i,j}$ stands for the strength of connection and $I_{ext}(t)$ is the external input from environment. Notably, if the matrix $C_{i,j}$ is random and sparse, we insert other degree of variability besides the microscopic one introduced above due to the structural arrangement of the network.

Once obtaining the time evolution of a single neuron in the interacting population, it is natural finding some global measurements to quantify the activity of Ω_N. One common measurements of network activity is the *instantaneous firing rate* that can be computed by the proportion of active neurons by counting the number of spikes $n_{act}(t; t + \Delta t)$ in a small time interval Δt and dividing by N. Further division by Δt yields

$$\nu(t) = \lim_{\Delta t \to 0} \frac{1}{\Delta t} \frac{n_{act}(t; t + \Delta t)}{N} = \frac{1}{N} \sum_{i=1}^{N} \sum_k \delta(t - t_{i_k}) \tag{1.12}$$

Looking at equation (1.12), global activity is defined by a population average. The advantage of this measurement is the possibility of comparing it with physiological data coming from non-invasive techniques like Electro-Encephalography (EEG). This method aims to record the electrical activity on the scalp that represent the macroscopic activity of the large brain region of the surface layers. Nevertheless, the EEG signals must propagate through various media, such as cerebrospinal fluid, cranium, and skin, and are therefore subject to filtering and diffusion phenomena across these media. More invasive techniques are able us to record the activity of limited and depth regions of the brain. Indeed, using deep electrodes, we can monitor electric potential in the extracellular space due to the activity of surrounding neurons in the sphere of 1 mm or by a few hundred microns [49]. This spatial-constraint potential takes the name of Local Field Potential (LFP) and includes the dynamics and structural arrangement of neurons, synapses and dendrites of investigated region. Because multiple neuronal processes contribute to the LFP, the signal is inherently ambiguous and more difficult to interpret than spikes train as well as its relation to single neuron variables like synaptic currents and membrane potentials. The situation is further complicated if we consider a spiking neural model where the space compartmental structure is neglected in order to be focus on dynamical properties.

The purpose of modelling the spiking neural model is to link the microscopic dynamics with the mesoscopic behaviour of one or more populations. Therefore, the main goal is to get the relation between neurons' variables and global quantities like instantaneous firing rate and LFP. Once obtain these signals, statistical and data analysis tools like spectrum analysis could shed light on possible synchrony activities and, more importantly, how the single elements are involved in this collective phenomenon.

Chapter 2

MODELS

In this chapter we describe in details the computational model used for our purpose. We want to emphasize that any choice we made is justified by the aim to describe neuron-glia interaction and its role into networks dynamics. For the modelling point of view it is crucial to understand the physiological mechanism that regulates the behavior of the studied systems. Therefore, starting from experimental data, the goal is to extrapolate knowledge about the system and to encode this information into the dynamical equations such that, the time evolution of variables in that model nicely reproduces experimental observations. Thus, the choice of the model reflects the level of detail we want to achieve for the microscopic description of synaptic transmission and the mesoscopic behaviour of both neuronal and neuro-glia networks. According to this, we adopt the Integrate and Fire approach for neuron dynamics and more physiological detailed model for synapses and astrocytes, such that Tsodyks-Markram for short-term plasticity and G-ChI for astrocytes. These allow us to deal with neurotransmitter and gliotransmitter concentration in extracellular space. The main disadvantage of these choice comes from the huge number of parameters that regulate in particular the astrocytes dynamics. However, due to their directly physiological meaning, it is easy to individuate the paramount parameters that could affect neuronal communication.

We describe in the following paragraph neuronal, synaptic and astrocytic models and their dynamical behavior through standard nonlinear analysis looking, for instance, at phase portrait and bifurcation plots. Last one is dedicate to the description of neuron-glia network.

2.1 Neurons

As already mentioned, the HH model describes the membrane potential in terms of sodium and potassium ions channel. Over the years, with the improvement of computational calculators, several ion channels are added to make the generation of the action potential more realistic. However, the growth of complexity suffers some limitations. Indeed, the essential nature of neuronal dynamics broadly remains hidden behind a multitude of factors and this is strictly related to huge parameter space that makes tedious any meaningful exploration of available phase space. The method of dimension reduction moves in the opposite direction, it tries to find the essential characteristic of neurophysiology to reproduce experimental data with the lowest possible number of variables and parameters. In this regard, models like FitzHugh-Nagumo [36] and Morris-Leclar [37] consistently describe

the neuron dynamics with only two variables, membrane potential and recovery variable.

Despite the complexity inherent in the generation of action potentials, in many cases, the conditions required for their initiation can be characterized quite straightforwardly: when the membrane potential reaches a certain threshold, a spike is initiated. In this setting lies the family of the Integrate-and-Fire model (IF). IF models only describe the sub-threshold membrane voltage $V(t)$, when the membrane potential crosses the threshold V_θ, the neuron fires causing the following consequences: the neuron potential is reset at a value V_r and the neuron cannot fire against for a refractory time τ_r. In our model, all the neurons are described by leaky integrate-and-fire (LIF), where the term *leaky* stands for the exponential decay of V with a characteristic time constant. The sub-threshold time course of membrane potential is described by the following ODE:

$$C_m \frac{dV}{dt} = g_l(E_l - V) + I_{syn}(t) + I_{ext}(t) \tag{2.1}$$

where C_m is the membrane capacitance and g_l is the membrane conductance. In addition, the model can take to account the synaptic current came from the activity of other neurons $I_{syn}(t)$ and the possible external current $I_{ext}(t)$. More precisely, a simple way of describing the time course of synaptic input is as a decaying exponential

$$I_{syn}(t) = \bar{I}_{syn}(t)\, s(t) \tag{2.2}$$

where $s(t)$ is the synaptic activity described in (1.10). In general, the neuronal susceptibility to being excitable depend on its present state. The conductance-based integrate-and-fire model takes into account this evidence due to the dependence of $\bar{I}_{syn}(t)$ on the difference between the membrane potential and the corresponding reversal potential E_{syn}:

$$I_{syn}(t) = g_{syn}\left(V(t) - E_{syn}\right) s(t) \tag{2.3}$$

Finally, considering the possibility of excitatory and inhibitory input, the complete model of conductance-based integrate-and-fire neuron connected with N_e exitatory and N_i inhibitory ones reads as:

$$\begin{aligned} C_m \frac{dV}{dt} &= g_l(E_l - V) + g_e(E_e - V) + g_i(E_i - V) + I_{ext}(t) \\ \frac{dg_e}{dt} &= -\frac{g_e}{\tau_e} + w_e \sum_{m=1}^{N_e} \sum_k \delta(t - t_{m_k}) \\ \frac{dg_i}{dt} &= -\frac{g_i}{\tau_i} + w_i \sum_{n=1}^{N_i} \sum_k \delta(t - t_{n_k}) \end{aligned} \tag{2.4}$$

where g_e and g_i are respectively the excitatory and inhibitory synaptic conductance with exponential time constant τ_e and τ_i. An arrival of spike at time t_{m_k} (t_{n_k}) from presynaptic excitatory (inhibitory) neurons m (n) causes an increase of postsynaptic conductance by w_e (w_i). Figure (2.1) illustrates an IF neuron described by equation (2.4)

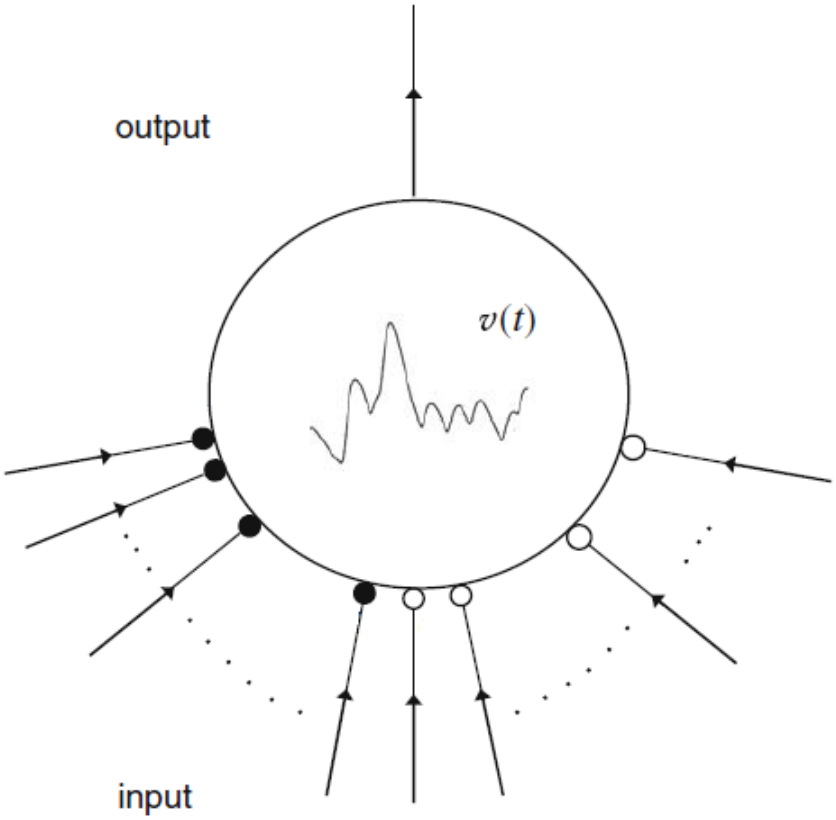

Figure 2.1: **Schematization of IF neuron**. Cartoon visualization of equation (2.4) with N_e excitatory (filled circles) and N_i inhibitory (open circles) current synapses. Each excitatory (inhibitory) synapse receives an input spike $\delta(t - t_{m_k})$ ($\delta(t - t_{n_k})$). Taken from Burkitt (2008) [38].

The integrate-and-fire neuron model is a single compartment model in which the spatial structure of the neuron associated with the dendrites is neglected. However, it is useful in understanding the basic properties of large networks of neurons and the implementation of synaptic plasticity is straightforward.

2.2 Synapses

In most model of neuronal systems, neurons are connected by chemical synapses, elements of the nervous system that allow the passage of signals from one neuron to another by releasing signaling molecules called neurotransmitters. The events leading to the opening of synaptic channels involve several steps. The action potential travels down the axon and terminates at many presynaptic sites, invading regions called synaptic terminals. These terminals contain calcium channels, when these are depolarized they cause release of calcium. The calcium then activates a calcium binding protein, which promotes transmitter release by binding to vesicles containing the transmitter. These "docked" vesicles release their transmitter into the synaptic cleft, which diffuses through the cleft, where it binds to various receptors on the postsynaptic neuron. These receptors open channels which either depolarize or hyperpolarize the neuron depending on the nature of the chemicals.

Neurotransmitters release can become quite complex to describe due to its probabilistic nature and the wild range of membrane receptors types. Furthermore, presynaptic stim-

ulation can lead to more vesicles becoming docked to the membrane, thus on the next presynaptic spike more transmitters is released than on the first spike. This increase is called potentiation or *synaptic facilitation*. Additionally, after several presynaptic spikes, the transmitter release per spike can decrease through various means, such as depletion, and take some time to recover. Decrease of transmitter over successive firings of action potentials is called *synaptic depression* [32].

To describe the dynamics of facilitation and depression of synaptic transmission, we adopt the phenomenological description of short-term plasticity first introduced by Tsodyks and Markram [44], by now indicated as TM model.

The TM model describes synaptic release (r_S) by the product of two factors: (i) the probability of neurotransmitter-containing vesicles to be available for release (x_S), and (ii) the probability of such vesicles to be effectively released by a presynaptic action potential (u_S), which correlates with intrasynaptic Ca^{2+} levels and the ensuing state of occupancy (activation) of the Ca^{2+} sensory of synaptic neurotransmitter exocytosis.

The variable u_S is zero at rest, when intrasynaptic Ca^{2+} concentration is low and the sensor for neurotransmitter exocytosis is only little bound, whereas it increases upon an action potential arriving at time t_k, mimicking increased of the fraction of binding synaptic sensor. In this interpretation the model assumes that a fraction u_0 of $1 - u_S$ of free binding sites of the sensor is instantaneously occupied by incoming Ca^{2+} ions and is following recovered at rate Ω_f. Thus, the dynimics of u_S is drived by

$$\frac{du_S^-}{dt} = -\Omega_f u_S^- + u_0 \sum_k (1 - u_S^-)\delta(t - t_k) \tag{2.5}$$

where the Dirac delta function $\delta(t - t_k)$ denotes the presynaptic spikes train and $u_S^- = u_S(t_k^-)$ denotes the values immediately before a generic action potential at time t_k.

Neurotransmitter resource in the presynaptic terminal are assumed limited and only a fraction of $x_S(t)$ of them is available for release. At rest, all resources are availeble, i.e. $x_S = 1$. When an action potential arrives, a fraction $u_S^+ = u_S^- + u_0(1 - u_S^-)$ of the resources is released into the cleft and is following reintegrated at rate Ω_d. The differential equation for time course of available neurotransmitter reads as

$$\frac{dx_S^-}{dt} = \Omega_d(1 - x_S^-) - \sum_k u_S^+ x_S^- \delta(t - t_k) \tag{2.6}$$

Accordingly, the fraction of neurotransmitter resources (r_S) is given by

$$r_S = u_S(t_k^+)\, x_S(t_k^-) = u_S^+\, x_S^- \tag{2.7}$$

Time evolution of variables in TM model is present in Figure(2.2)

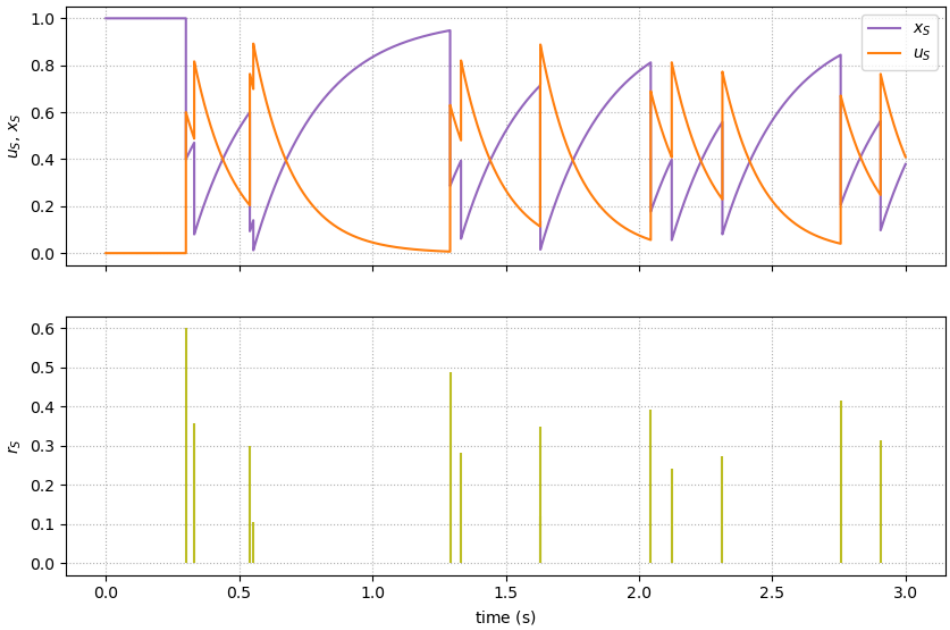

Figure 2.2: **Dynamical behavior of variables in TM model**. Time evolution of x_S (purple) and u_S (orange) for Poisson presynaptic firing rate of 4 spk/s. Time simulation covers 3 second, integration steps is 0.05 ms. Parameters as in table in Appendix B.1

Equations (2.5) and (2.6) compose the TM model where the parameter u_0 coincides with the value that u_S reaches at resting condition immediately after first action potential of a series. When presynaptic firing rate is low than facilitation and depression time constant, i.e. $\nu_S \ll \Omega_f, \Omega_d$, synaptic variables reach their initial values and, as a consequence, the dynamics is equal to the total absence of plasticity. Then, in this case, the release probability from synapses equals u_0. On the other hand, intense presynaptic firing rate provides strong depletion of resources that drastically reduce neurotransmitter exocytosis.

The neurotransmitter's time course in the synaptic cleft must be tacking into account to complete our description of synaptic transmission. We assume a total vesicular neurotransmitter concentration of Y_T, thus the released concentration in the synaptic cleft is equal to $Y_{rel}(t_i) = \rho_c Y_T r_S(t_k)$, where ρ_c represents the ratio between vesicular and synaptic cleft volumes. The time course of synaptically released neurotransmitters in the cleft (Y_S) depends on several mechanisms, including clearance by diffusion, uptake and degradation. In the simplest approximation, the contribution of these mechanisms to glutammate time course in the cleft may be modelled by a first-order degradation reaction of characteristic time so that [12]:

$$\frac{dY_S}{dt} = -\Omega_c Y_S + \sum_k Y_{rel}\delta(t - t_k) \tag{2.8}$$

2.3 Astrocytes

Among all possible second messengers in astrocytic cytosol, Ca^{2+} and inositol 1,4,5-trisphosphate (IP_3) are the most studied ones and are the core of most glio-computational models. For Ca^{2+}, influx usually occurs via two principal pathways: inflow from the extracellular medium through Ca^{2+} channels located in the cell membrane and release from internal stores (as endoplasmatic reticulum) via IP_3R, membrane channel binding with IP_3. Removal of Ca^{2+} from the cytosol also occurs in two principal ways: it is pumped out of a cell and is sequestered back into the internal store. In addiction, Ca^{2+} ions can also passively leak from the internal store into the cytosol.

In astrocytes, the primary mechanism about influx is considered the IP_3-dependent calcium release from endoplasmatic reticulum (ER). Morover IP_3 concentration into the cytosol strongly depends on Ca^{2+}, thus this mechanims is called Ca^{2+}-induced Ca^{2+}-release (CICR). Classical models for a biophysically realistic cytosolic Ca^{2+} oscillation was developed by De Young and Keizer [42]. It mimics the molecular subunit configuration of the IP_3R to reflect the activation/inactivation sequence of the channel resulting from the binding of Ca^{2+} and IP_3. In particular, the model assumes that the IP_3R is composed of three independent and identical subunits, each state of the subunit is given by X_{ikj} wiht $i, k, j = 0, 1$, where the first index refers to the IP_3 binding site, the second to the Ca^{2+}-activated site and the third to the Ca^{2+} -inactivated site. Therefore the model consists of six ODEs, one for each subunit, and one differential equation for Ca^{2+} dynamics:

$$\begin{aligned}
&\frac{dX_{110}}{dt} = [k_1 I X_{010} - k_1 X_{110}] + [k_{-2} X_{111} - k_4 C X_{110}] + [k_5 C X_{100} - k_{-5} C X_{110}] \\
&... \\
&\frac{dX_{000}}{dt} = [k_{-1} X_{100} - k_1 I X_{000}] + [k_{-4} X_{001} - k_4 C X_{000}] + [k_{-5} X_{010} - k_5 C X_{000}] \\
&\frac{dC}{dt} = \rho_A(\Omega_C X_{110}^3 + \Omega_L)(C_{ER} - C) - O_P \mathcal{H}_2(C, K_P)
\end{aligned} \tag{2.9}$$

where $C_{ER} = (C_T - C)/\rho_a$ denotes Ca^{2+} in the ER, ρ_a is the volume ratio between the ER and the cytosol, and C_T is the total concentration of Ca^{2+}, whereas k_{-i} (k_i) are the rate (rate/moles) of reactions.

The complexity of the DYK model consisting of huge phase space provides motivation to simplify the model with the retention of its essential properties. One simplification was suggested by Li and Rinzel [43] who have shown that the original full model can be reduced to just two ODEs. The dimension reduction is based on experimental evidence that IP_3 and Ca^{2+} bind quickly to the activating sites giving rise to the assumption that the receptor is in a quasi-steady-state with respect to IP_3 binding and Ca^{2+} activation. Therefore it could be possible to mathematical treat Equations (2.9) and write down the reduced model with one differential equation for Ca^{2+} dynamics (C) and other one for inactivation variable (h) account for the three gating reactions, respectively, IP_3-binding, activating Ca^{2+}-binding and Ca^{2+}-dependent inactivation of the receptor [7]:

$$\begin{aligned}
\frac{dC}{dt} &= J_r + J_l - J_p \\
\frac{dh}{dt} &= \frac{h_\infty - h}{\tau_h}
\end{aligned} \tag{2.10}$$

where $h_\infty = \frac{Q_2}{Q_2+C}$, $\tau_h = \frac{1}{O_2(Q_2+C)}$ and $Q_2 = d_2\frac{I+d_1}{I+d_3}$ and d_i is intimate relate with k_i and k_{-i} (see Appendix B for details about parameters)

According to above consideration, calicium dynamics is described by three different fluxes. $J_l(C)$ stands for nonspecific leak current that is assumed to the Ca^{2+} gradient across the ER membrane by Ω_L, the maximal rate of Ca^{2+} leakage from the ER:

$$J_l(C) = \Omega_L(C_T - (1+\rho_A)C) \tag{2.11}$$

$J_p(C)$ represents the SERCA pump flux and can be taken as an instantaneous function of C by assuming Michaelis-Mentena kinetics description [45] with exponent 2:

$$J_p(C) = O_P\,\mathcal{H}_2(C, K_P) \tag{2.12}$$

where O_P is the maximal rate of Ca^{2+} uptake by the pump and K_P is the SERCA Ca^{2+} affinity, that is the Ca^{2+} concentration at which the pump operates at half of its maximal capacity, and $\mathcal{H}_2(C, K_P)$ is the Hill function [1]

$J_r(C, h, I)$ is the current through the IP_3R channels, Li and Rinzel proposed the following equation for this terms:

$$J_r(C, h, I) = \Omega_C m_\infty^3 h_\infty^3 (C_T - (1+\rho_A)C) \tag{2.13}$$

with the channel open probabilty is given by $m_\infty^3 h_\infty^3$, where $m_\infty^3 = \mathcal{H}(I, d_1)\mathcal{H}(I, d_1)$. The power of 3 was directly suggested by experimental data. I stands for the intercellular IP_3 concentration and Ω_C is the maximum channel permeability. The dynamics of the inactivation variable h is reminiscent of that of the gating variables in the Hodgkin-Huxley model of nerve membrane and its dependence on C is embadded into the parameters h_∞ and τ_h in highly nonlinear fashion.

It is important to underline that the strong of Li-Rinzel model is the ability to reproduce the same dynamical behavior of DeYoung-Keizer model and the same kind of physiological oscillation [14]. In particular it can reproduce both amplitude (AM) and frequency (FM) modulation depend on SERCA uptake parameters K_P as illustate respectively in Figure(2.3) and Figure(2.4).

[1] The binding reaction of n molecules of a ligand A to a receptor is well described by a Hill function $\mathcal{H}_n(A, B) = \frac{A^n}{A^n+B^n}$ where n is the Hill coefficient that quantifies the cooperativity among multiple ligand-binding sites and B is the receptor affinity for the ligand.

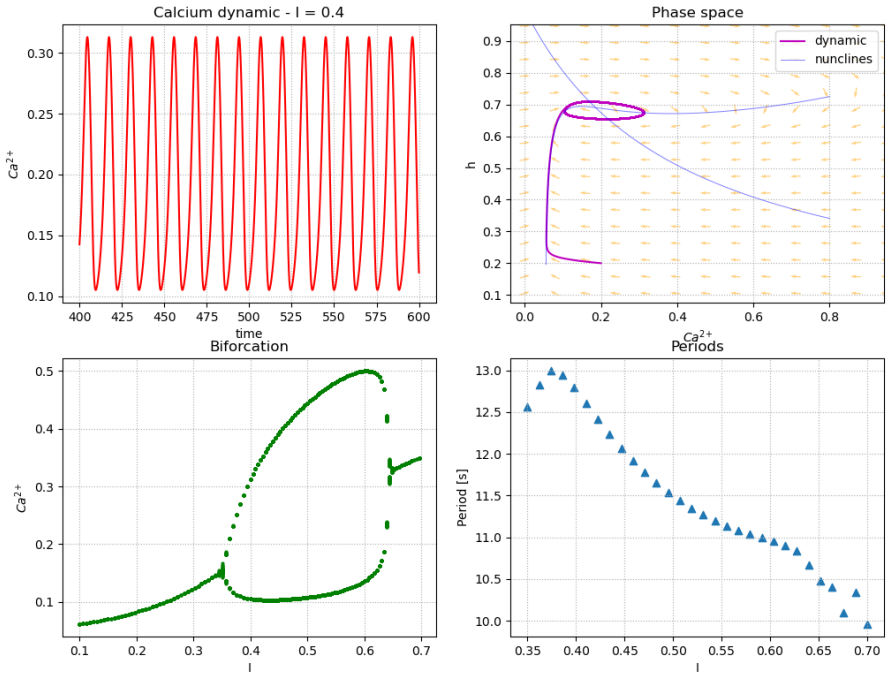

Figure 2.3: **Amplitude modulation (AM) encoding mode generated by the Li-Rinzel model.**(Top left) the shape of calcium oscillation is quasisinusoidal, the phase portrait (Top right) show a single intersection of nunclines, the unstable fixed point. Changing the parameters I, qualitatively changes of dynamical is illustates in bifurcation plot (Bottom left) where the steady state changes its nature through Hopf bifurcations (cit glutammate). Time simulation covers 600 second, only data after 400 second are taken to compute bifurcation diagram. Parameters as in table in Appendix B.2

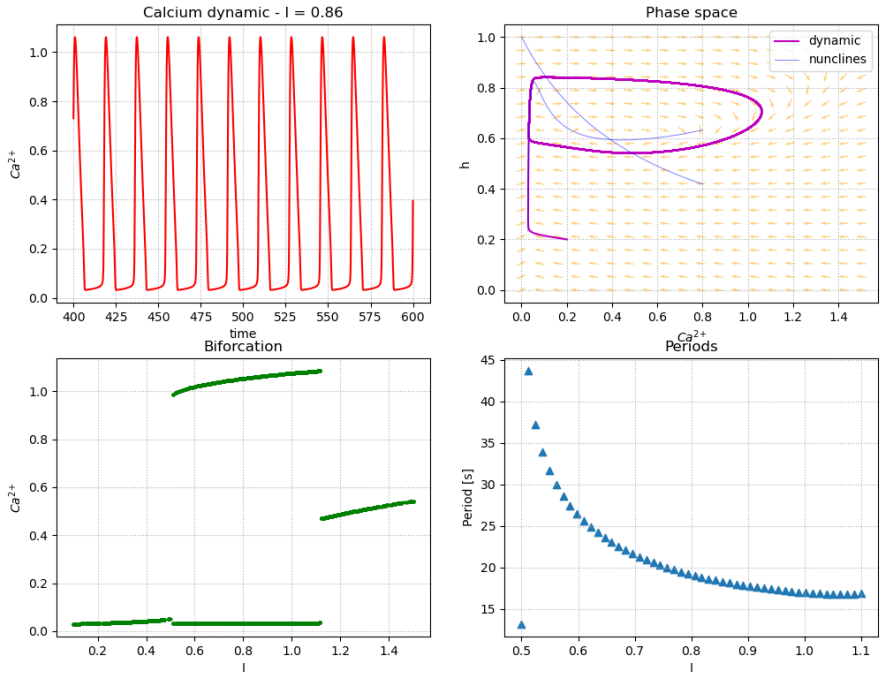

Figure 2.4: **Frequency modulation (FM) encoding mode generated by the Li-Rinzel model**. (Top left) the shape of calcium oscillation has a pulse-wise fashion. The number of stable fixed pints change with the values of I according to the sandle-node bifurcations (cit) as illustate in bifurcation plot (bottom left). for $I = 0.86$ the phase portrait (Top right) show a single intersection of nunclines. The nature of frequency modulation is clear looking at the range of periods with respects to I (bottom right). Time simulation covers 600 second, only data after 400 second are taken to compute bifurcation diagram. Parameters as in table in Appendix B.2

The limitation of Li-Rinzel model is that assumes IP_3 does not vary with time nor depend on the other dynamical variable, i.e. in Equation (2.10) its concentration is a parameter of the model as emphasized in above dynamical behavior analysis. Evidences suggest IP_3 concentration depends on both intracellular Ca^{2+} and extracellular chemicals. For instance, glutammate concentration at the extracellular side of the astrocyte membrane determines the degree of activation of mGluRs, membrane channels directly linked to intracellular IP_3 concentration.Accordingly, IP_3 should be an addiction variable in the model.

To update the Li-Rinzel model according to this consideration, it is need tacking to account both endogenous and exogenous production as well as its degradation mechanism, only such modeling can provide a realistic account of astrocytic Ca^{2+} variations induced by nearby synaptic inputs.

Astrocytic IP_3 concentration is regulated by the complex Ca^{2+}-modulated interplay of enzymatic production by Cβ (J_β) and Cδ (J_δ) and degradation by IP_3 3-kinase (J_{3K}) and inositol polyphosphatase 5-phosphatase (J_{5P}) [14]. To reproduce experimental observations, two possible ways to trigger IP_3 production must be tacking into account. One is by synaptic stimulation of astrocytic metabotropic receptors which starts phospholipase Cβ-mediated IP_3 production, modeled by making J_β proportional to the activated fraction of these receptors (denoted hereafter by Γ_A). The other way is to include a further J_{ex} term for constant IP_3 production by an exogenous source of stimulation such as, for example,

IP_3 uncaging or intracellular diffusion from subcellular regions far from the CICR site. Mass balance equation for IP_3 concentration $I(t)$ reads as:

$$\frac{dI}{dt} = J_\beta + J_\delta - J_{3K} - J_{5P} + J_{ex} \tag{2.14}$$

For our porpouse we used biophisical modeling approach fully described in (cita ch5) based on the assumption of Michaelis-Menten enzyme kinetics to effectively describe the wild range of complex chemical reactions that leads to IP_3 synthesis. Each fluxes in Equation (2.14) are described by the following nonlinear expression:

$$\begin{aligned} J_\beta &= O_\beta \Gamma_A \\ J_\delta(I) &= O_\delta(1 - \mathcal{H}_1(I, \kappa_\delta))\mathcal{H}_2(C, K_\delta) \\ J_{5P} &= \Omega_{5P} I \\ J_{3K} &= O_{3K}\mathcal{H}_4(C, K_D) \end{aligned} \tag{2.15}$$

The dynamics of the fraction of bound receptors needs to complete this description. Γ_A is defined as $\Gamma_A = [R^*]\,]/[R]_T$, with $[R]_T = [R] + [R^*]$ being the total receptor concentration at the site of IP_3 production, thus its dynamics depends on the cascade of reactions drives [R] and [R*] [8].

Finally, putting together (2.10), (2.14) and (2.15) leads to the so called *G-ChI model* for IP_3/Ca^{2+} signaling:

$$\begin{aligned} \frac{d\Gamma_A}{dt} &= O_N Y_S(1 - \Gamma_A) - \Omega_N\left(1 + \zeta\mathcal{H}_1(C, K_{KC})\right)\Gamma_A \\ \frac{dC}{dt} &= J_r(C.h, I) + J_l(C) - J_p(C) \\ \frac{dh}{dt} &= \frac{h_\infty(C, I) - h}{\tau_h(C, I)} \\ \frac{dI}{dt} &= J_\beta(\Gamma_A) + J_\delta(C, I) - J_{3K}(C, I) - J_{5P}(I) \end{aligned} \tag{2.16}$$

where Y_S stands for the neurotrasmitter concentration in the periastrocytic space. Figure (2.5) illustrates G-ChI model can reproduce, like LR one, calcium oscillation in the sinusoidal-like fashion modality.

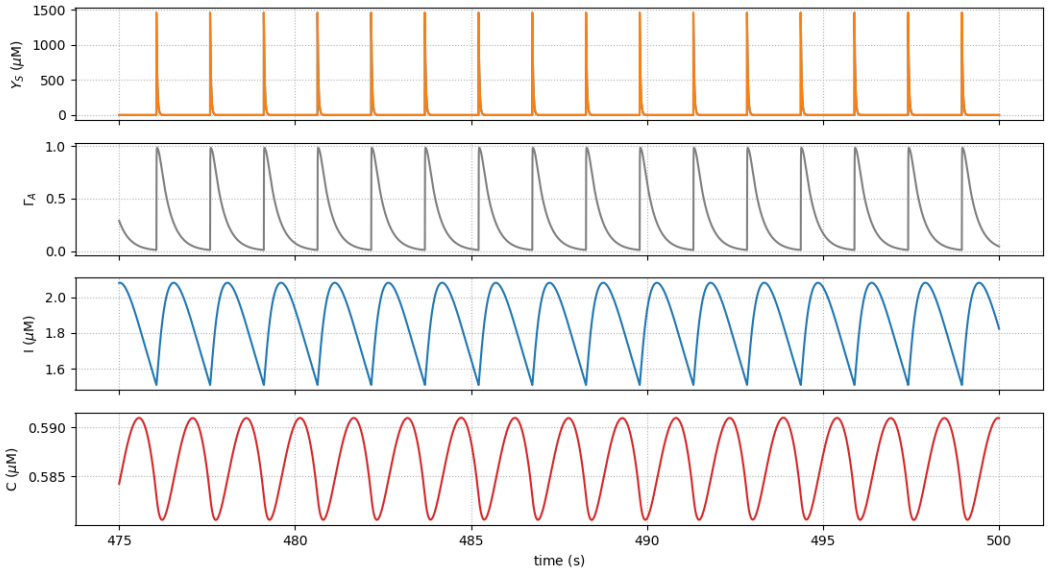

Figure 2.5: **Astrocytic variables dynamics in G-ChI model**. Synaptically activated astrocyte described by G-ChI model. Constant presynaptic firing rate of 0.6 Hz drives the neurotransmitter release and, according to TM model, its concentration upon each action potential arrivals (Top panel)notably, there are present either depression neither facilitation because of the regular inter-spike interval (ISI). The time course of astrocityc membrane receptors Γ_A deeply effects the time evolution of I. Importantly, for this combination of parameters, Ca^{2+} oscillations (bottom panel) are clearly visible as in AM of LR model in figure(2.3). Time simulation covers 500 seconds, only data after 475 seconds are plotted, with integration steps of 0.5 ms. Parameters as in table in Appendix B.2, $O_\beta = 3.2$ μM and $O_\delta = 0.6$ μM

This is the starting point to describe and analyze the neuro-glia interaction at the microscopic level. However, equation (2.16) provides only the synaptic activation of the astrocytic variable and, to consider also the gliomodulation of synaptic activity, we may describe the exocytosis and the time course of gliotransmitters in the synaptic cleft.

A large amount of evidence suggest that gliotransmitter exocytosis from astrocytes share several similarities with its synaptic homologous. Astrocytes indeed possess vesicular compartments that are competent for exocytosis of glutammate, fusion with plasma membrane, trafficking and recycling of glutammate-containing vesicles have also been observed in astrocytes which are indicative of quantal exocytotic release of these gliotransmitters. The the above arguments are the based of gliotransmitter exocytosis from astrocytes proposed by De Pittà in [10]. Astrocytic glutammate exocytosis is modeled akin to synaptic glutammate release, assuming that a fraction $x_A(t)$ of gliotransmitter resources is available for release at any time. Then, every time t_j that astrocytic Ca^{2+} increases beyond a threshold concentration C_θ, a fraction of readily releasable astrocytic glutammate resources, that is, $r_A(t_j) = U_A x_A(t_j^-)$, is released into the ECS and later reintegrated at rate Ω_A. Hence x_A evolves according to:

$$\frac{dx_A}{dt} = \Omega_A(1 - x_A) - \sum_j r_A \delta(t - t_j) \tag{2.17}$$

where the Delta function denotes a Gliotransmitter release event (GRE) at time t_j. Note that U_A in $r_A(t_j) = U_A x_A(t_j^-)$ is the astrocytic analogous of the synapse's basal release probability in (2.5).

Similarly to synaptic case, it is possible to estimate the contribution to glutammate concentration in the ECS space (G_A), resulting from a quantal glutammate release event by the astrocyte at $t = t_j$, as $G_{rel}(t_j) = \rho_e G_T r_A(t_J)$, where G_T represents the total vesicular glutammate concentration in the astrocyte and ρ_e is the volume ratio between glutammate-containing astrocytic vesicles and periastrocytic space. Then, assuming a clearance rate of glutammate of Ω_e , the time course of astrocyte-derived glutammate in the ECS comprised between the astrocyte and the surrounding synaptic terminals is given by:

$$\frac{dG_A}{dt} = -\Omega_e G_A + \sum_j G_{rel}\delta(t - t_j) \tag{2.18}$$

2.3.1 Gliotransmission modulation of synaptic release

Gliotransmission is the phenomenon by which glial activity influences the synaptic release and the underlying biological mechanisms follow the aforementioned synaptic modulation of astrocytic calcium oscillations. Depending on the type of gliotransmitter and the type of bound presynaptic receptors, gliotransmission can either increase or decrease synaptic release. All receptors, independently of the type, ultimately regulate intrasynaptic Ca^{2+} levels, thereby modulating the release probability of neurotransmitter-containing synaptic vesicles. It is important to note that this kind of modulation does not require synaptic activation by action potentials and is observed even in basal conditions.

Based on this argument, an ansatz can be made whereby gliotransmitter modulation of synaptic release can be reproduce by the TM synaptic model, making the variable u_S in (2.5) depend on gliotransmitter dynamics in the ECS, i.e. G_A in equation (2.18). The model arises from this hypothesis is fully reviewed in [10].

It may be assumed that basal synaptic release probability u_0 is not constant, but rather it is a function of G_A through the fraction Γ_S of presynaptic receptor that are activated by released gliotransmitter molecules

$$u_0 \equiv u_0(G_A) = u_0(\Gamma_S(G_A)) \tag{2.19}$$

In the absence of quantitative physiological data, the function $u_0(\Gamma_S)$ can be taken analytic around zero that its firts-order expantion is considered accordingly:

$$u_0(\Gamma_S) \simeq u_0(0) + u_0'(0)\Gamma_S + O(\Gamma_S^2) \tag{2.20}$$

The zeroth-order term $u_0(0) = U_0^*$ corresponds to the value of u_0 in the absence of astocyte, hence this approximation falls back to the classic TM model. To express $u_0{}'(0)$ instead, it may be noted that both $u_0(\Gamma_S)$ and Γ_S are defined in the interval [0, 1], so that $u_0(\Gamma_S)$ must either increase or decrease with Γ_S depending on whether gliotransmission stimulates or inhibits synaptic release. In the simplest scenario, the choice of $u_0 = \alpha - U_0^*$ can be made so that, neglecting the terms of $O(\Gamma_S^2)$ in equations (2.20) ultimately provides

$$u_0(\Gamma_S) = U_0^* + (\alpha - U_0^*)\Gamma_S \tag{2.21}$$

The parameter α in the above equation lumps in a phenomenological way information on the effect of gliotransmission on synaptic release. For $0 \leq \alpha < U_0^*$, u_0 decreases with Γ_S, consistently with the *release-decreasing* effect of gliotrasmission on synaptic release. This could be the case of astrocytic glutammate targeting presyaptic kainate

receptors or group II/III metabotropic receptors [46]. For $U_0^* < \alpha \leq 1$, u_0 increase with Γ_S, consistent with a *release-increasing* effect of gliotrasmission on synaptic release, like in the case of glutammate in association with presynaptic NMDA receptors of group I metabotropic receptors . Finally, for $\alpha = U_0^*$, it is $u_0 = U_0^*$, independently of Γ_S. This case corresponds to *occlusion*, that is no net effect of gliotransmission on synaptic release due to the simultaneous activation of stimulatory and inhibitory receptors that may be co-expressed at the same synaptic terminal.

Finally, the presynaptic receptor dynamics are assumed to complete the model. The pool of presynaptic receptors target with gliotransmitters is composed of a fraction of bound receptors Γ_S and a complementary fraction $1 - \Gamma_S$ of available ones, thus Γ_S evolves according to

$$\frac{d\Gamma_S}{dt} = O_G G_A (1 - \Gamma_S) - \Omega_G \Gamma_S \tag{2.22}$$

where O_G and Ω_G denote rate constants loosely related with rise and decay of the modulation of synaptic release by gliotransmitters.

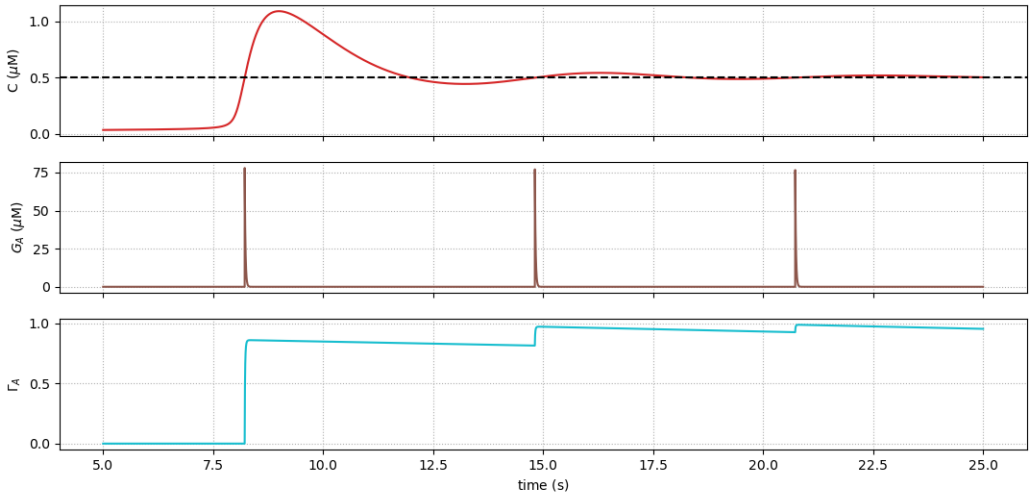

Figure 2.6: **Gliorelease event (GRE)**. (Top panel) Astrocityc calcium oscillation (red solid line) across the threshold values (black dashed line) drives the release of gliotrasmitters. Time course of gliotransmitters in extracellular (middle panel) space and presynaptic receptors (bottom panel). The sawtooth-shaped Γ_S increase is a consequence of the large difference between timescales of rise and decay of the gliotransmitter effect on synaptic release, since $O_G G_A \ll \Omega_G$. Time simulation covers the time window 5.0 - 25.0 seconds, with integration steps of 0.5 ms. Parameters as in table in Appendix B.2, $O_\beta = 0.5$ μM and $O_\delta = 1.2$ μM

In conclusion, in these sections, we have underlined the main physiological and computational aspects of the two pathways of interaction between neurons (more precisely the synapses) and astrocytes. Theese will be the core of tripartite synapse, the the main topic of the following chapter.

2.4 Neuro-Glia Network

For the core of our Neuro-Glia network, we chose an excitatory/inhibitory spiking neural network with inter and intrapopulation connections. This network is composed of $N = N_e + N_i = 4000$ neurons, $N_e = 3200$ excitatory and $N_i = 800$ inhibitory ones. The network connectivity among neurons is described by a random and sparse matrix $C_{l,l}$ with $l = 1, ..., N$, in particular, the connecting probability with an excitatory neuron is $p_e = 0.05$ whereas it is $p_i = 0.2$ with an inhibitory one, such that each cell receives, on average, the same amount of recurrent input equals to $N_x\, p_x$ with $x = e, i$. Because the inhibitory synaptic strength is 20 times greater than the excitatory one (see parameters values in Appendix B), the entire network has a strong inhibitory recurrent connection. Recurrent connections are provided by short-term plasticity synapses, hence the synaptic strengths w_e and w_i are modulated by the factor r_S in 2.7. All neurons are described by conductance-based leaky integrate and fire described in (2.4) where the external input comes from a pool of excitatory neurons thereby the frequency $\nu_{ext}(t)$ characterizes the input stimuli. Moreover, to describe the neural variability, each spikes train of external input is a different realization of Poisson process[2].

The membrane potential of neuron l in the excitatory/inhibitory network ($V^{(l)}$) evolves according to:

$$\begin{aligned}
C_m \frac{dV^{(l)}}{dt} &= g_l(E_l - V^{(l)}) + g_e^{(l)}(E_e - V^{(l)}) + g_i^{(l)}(E_i - V^{(l)}) + g_{ext}^{(l)}(E_e - V^{(l)}) \\
\frac{dg_e^{(l)}}{dt} &= -\frac{g_e^{(l)}}{\tau_e} + \sum_{m=1}^{N} C_{l,m}\, w_e \sum_k r_S(t_{m_k})\delta(t - t_{m_k}) \\
\frac{dg_i^{(l)}}{dt} &= -\frac{g_i^{(l)}}{\tau_i} + \sum_{n=1}^{N} C_{l,n}\, w_i \sum_k r_S(t_{n_k})\delta(t - t_{n_k}) \\
\frac{dg_{ext}^{(l)}}{dt} &= -\frac{g_{ext}^{(l)}}{\tau_e} + \sum_{p=1}^{N_{ext}} w_e \sum_k \delta(t - t_{p_k})
\end{aligned} \tag{2.23}$$

As we describe in the previous section, the neuron-glia interaction appears at the synaptic level and it is quite noticeable that the situation is further complicated when we have to treat gliomodulation at the network level. Precisely, experimental evidence suggests hippocampal astrocyte has been estimated to contact about 100.000 synapses [50] moreover, astrocytes organize in complex networks through connections by gap junction channels that are regulated by extra- and intracellular signals [9]. Theoretical and computational efforts about such a complete system go beyond the purpose of the present thesis. Nevertheless, we consider a network which can contain information as close to the current physiological knowledge as possible: each astrocyte is available to take part in several tripartite synapses while we only neglect the connectivity among non-neural cells. Starting from the model described in [11], we consider $N_a = N = 4000$ astrocytes whereby each of them forms a connection with all the excitatory synapses ingoing into a

[2]Poisson distribution satisfies the following propriety: let X and Y be independent Poisson random variables with parameters ν_1 and ν_2, respectively and the process defined as a sum of X and Y , i.e. Z = X+Y. Then Z is a Poisson random variable with $\nu = \nu_1 + \nu_2$. We indicate with ν_{ext} the sum of all external neurons

postsynaptic neurons, thus neurons-astrocytes connectivity is described by a matrix A_{l,m_l}, where $l = 1, ..., N_a$ and $m_l = 1, ..., N_e^{syn}$, the total number of excitatory synapses

$$\begin{aligned}
C_m \frac{dV^{(l)}}{dt} &= g_l(E_l - V^{(l)}) + g_e^{(l)}(E_e - V^{(l)}) + g_i^{(l)}(E_i - V^{(l)}) + g_{ext}^{(l)}(E_e - V^{(l)}) \\
\frac{dg_e^{(l)}}{dt} &= -\frac{g_e^{(l)}}{\tau_e} + \sum_{m=1}^{N} C_{l,m}\, w_e \sum_k A_{l,m_l}\, r_S(t_{m_k})\, \delta(t - t_{m_k}) \\
\frac{dg_i^{(l)}}{dt} &= -\frac{g_i^{(l)}}{\tau_i} + \sum_{n=1}^{N} C_{l,n}\, w_i \sum_k r_S(t_{n_k})\, \delta(t - t_{n_k}) \\
\frac{dg_{ext}^{(l)}}{dt} &= -\frac{g_{ext}^{(l)}}{\tau_e} + \sum_{p=1}^{N_{ext}} w_e \sum_k \delta(t - t_{p_k})
\end{aligned} \tag{2.24}$$

the term $r_S(t_{m_k})$ lumps all the information about astrocytic regulation through equations (2.21) and (2.22).

Chapter 3

SYNAPTIC TRANSMISSION

The present chapter illustrates the possible realization of signalling transmission through the chemical synapses and how the frequency of incoming spikes train drives the release of neurotransmitters into the synaptic cleft. Accordingly, to have a broad and overreaching comprehension of these phenomena, we start to analyse the well-described picture of bipartite synapses in the presence of short-term plasticity [18, 19] and the gliomodulation effects in the heterosynaptic connection [10]. Thereafter we deepen the more realistic scenario of bidirectional coupling between astrocyte and neurons, the homosynaptic connection. More precisely, methods of nonlinear systems theory lead us to a plausible mean field approximation thereby we can recognize astrocyte parameters that affect in a greater way signalling transmission.

3.1 Bipartite Synapse

The phenomenological model of bipartite synapse introduced in 2.2 can be used to analyse the way activity of a large population of presynaptic neurons is transmitted to the postsynaptic target. Indeed, the TM model can be mathematically manipulated to derive a mean field description to get quantitative insights into the synaptic transmission.

The dynamics driven by generic spikes train is completely described by the following set of equations:

$$\begin{aligned} \frac{du_S^-}{dt} &= -\Omega_f u_S^- + u_0 \sum_k (1 - u_S^-)\delta(t - t_k) \\ \frac{dx_S^-}{dt} &= \Omega_d(1 - x_S^-) - \sum_k u_S^+ x_S^- \delta(t - t_k) \\ u_S^+ &= u_S^- + u_0(1 - u_S^-) \end{aligned} \tag{3.1}$$

that is a nonlinear dynamical system of two ODEs. Substituting the third expression into the first leads to more useful form for next steps of mean field derivation:

$$\begin{aligned} \frac{du_S^+}{dt} &= \Omega_f(u_0 - u_S^+) + u_0 \sum_k (1 - u_S^+)\delta(t - t_k) \\ \frac{dx_S^-}{dt} &= \Omega_d(1 - x_S^-) - \sum_k u_S^+ x_S^- \delta(t - t_k) \end{aligned} \tag{3.2}$$

To simplify the notation, the variables are redefined without the apexes. Let's consider n_S trials of stimulation of a synapse by trains of action potentials of equal length

and same statistics, delivered to the synapse at identical initial conditions. The trial-averaged synaptic dynamics is described by equations (3.2) in term of mean quantities $\bar{u_S} = 1/n_S \sum_{l=1}^{n_s} u_{S_l}$ and $\bar{x_S} = 1/n_S \sum_{l=1}^{n_s} x_{S_l}$:

$$\begin{aligned} \frac{d\bar{u_S}}{dt} &= \Omega_f(u_0 - \bar{u_S}) + \frac{u_0}{n_S}\sum_{l=1}^{n_S}\sum_k (1 - u_{S_l})\,\delta(t - t_{l_k}) \\ \frac{d\bar{x_S}}{dt} &= \Omega_d(1 - \bar{x_S}) - \frac{1}{n_S}\sum_{l=1}^{n_S}\sum_k u_{S_l}x_{S_l}\,\delta(t - t_{l_k}) \end{aligned} \tag{3.3}$$

where $\delta(t - t_{l_k})$ represents the arrival of the k-th spike of trial l. In a small time interval Δt, the above equations can be rewritten in terms of finite differences as:

$$\begin{aligned} \bar{u_S}(t + \Delta t) - \bar{u_S}(t) &= \Omega_f(u_0 + \bar{u_S})\Delta t + \frac{u_0}{n_S}\sum_{l}^{n_S}(1 - u_{S_l})\,\Delta_l(\Delta t) \\ \bar{x_S}(t + \Delta t) - \bar{x_S}(t) &= \Omega_d(1 - \bar{x_S})\Delta t - \frac{1}{n_S}\sum_{l}^{n_S} u_{S_l}x_{S_l}\,\Delta_l(\Delta t) \end{aligned} \tag{3.4}$$

where $\Delta_l(\Delta t) = \sum_k \delta(t - t_{l_k})\Delta t$ is the number of spikes in the time interval Δt for the l-th trial and it is a stochastic quantity. In sections 1.4.2 and 1.5, we have already mentioned that individual neurons in vivo fire irregularly at all rates, reminiscent of a Poisson process. Mathematically, the Poisson assumption means that, at each moment, the probability that a neuron fires equal the neuron's instantaneous firing rate and is independent of the timing of previous action potentials. Then, assuming that the n_S trains are different realizations of the same Poisson process with average rate $\nu_S(t)$, equations (3.4) can be averaged in time over a proper Δt. In particular, thanks to the Poisson hypothesis, the variable u_S, x_S, $u_S x_S$ and $\Delta_l(\Delta t)$ can be considered independent and thus be averaged independently. Therefore, taking Δt of a order of several intervals between spikes, but shorter than longest time scale in the system ($1/\Omega_d$ and $1/\Omega_f$), the time average, denoted by $\langle\cdot\rangle$, of $\Delta_l(\Delta t)$ can be estimate by $\Delta_l(\Delta t) = \nu_S(t)\Delta t$. Accordingly,

$$\begin{aligned} \langle\bar{u_S}(t + \Delta t)\rangle - \langle\bar{u_S}(t)\rangle &= \Omega_f(u_0 - \langle\bar{u_S}\rangle)\Delta t + \frac{u_0}{n_S}\sum_{l}^{n_S}(1 - \langle u_{S_l}\rangle)\,\nu_S(t)\Delta t \\ \langle\bar{x_S}(t + \Delta t)\rangle - \langle\bar{x_S}(t)\rangle &= \Omega_d(1 - \langle\bar{x_S}\rangle) - \frac{1}{n_S}\sum_{l}^{n_S}\langle u_{S_l}x_{S_l}\rangle\,\nu_S(t)\Delta t \end{aligned} \tag{3.5}$$

Finally, divided by Δt yields

$$\begin{aligned} \frac{d\langle\bar{u_S}\rangle}{dt} &= \Omega_f(u_0 - \langle\bar{u_S}\rangle) + u_0(1 - \langle\bar{u_S}\rangle)\,\nu_S(t) \\ \frac{d\langle\bar{x_S}\rangle}{dt} &= \Omega_d(1 - \langle\bar{x_S}\rangle) - \langle\bar{u_S}\rangle\langle\bar{x_S}\rangle\,\nu_S(t) \end{aligned} \tag{3.6}$$

that is a nonlinear and nonautonomous set of two ODEs with respect to $\nu_S(t)$ and describe the dynamics of average synaptic variables. In general, it is possible to resolve analytically the first equations and then, putting the results in the second, give the solution of the whole system [10]. However, when the presynaptic firing rate is constant in time, namely in the case of a homogeneous Poisson process with rate ν_S, the system becomes autonomous

and it is possible to evaluate the steady states. In particular, the intersection of nunclines, the ensemble of point in which vector field is null, provides the fixed points for the systems:

$$\begin{aligned} \langle \bar{u_S} \rangle &= \frac{u_0(\Omega_f + \nu_S)}{\Omega_f + \nu_S\, u_0} \\ \langle \bar{x_S} \rangle &= \frac{\Omega_d}{\Omega_d + \langle \bar{u_S} \rangle\, \nu_S} \end{aligned} \tag{3.7}$$

the mean value of release probability is given by the product of the steady states in (3.7)

$$\langle \bar{r_S} \rangle = \frac{u_0 \Omega_d (\Omega_f + \nu_S)}{(\Omega_f + \nu_S\, u_0)(\Omega_d + \langle \bar{u_S} \rangle\, \nu_S)} \tag{3.8}$$

This analytical approximation solution is able us to estimate the behaviour with extreme values in two limit scenarios. For low firing rate, i.e. $\nu_S \to 0$, the probability of release tends to u_0 and the available neurotransmitter resources tends to 1, thus the $r_S \to 1 \cdot u_0 = u_0$. Conversely for high firing rate, i.e. $\nu_S \to +\infty$, u_S tends to 1 and x_S tends to 0, therefore the average values of neurotransmitter is 0 (solid line in Figure (3.1)).

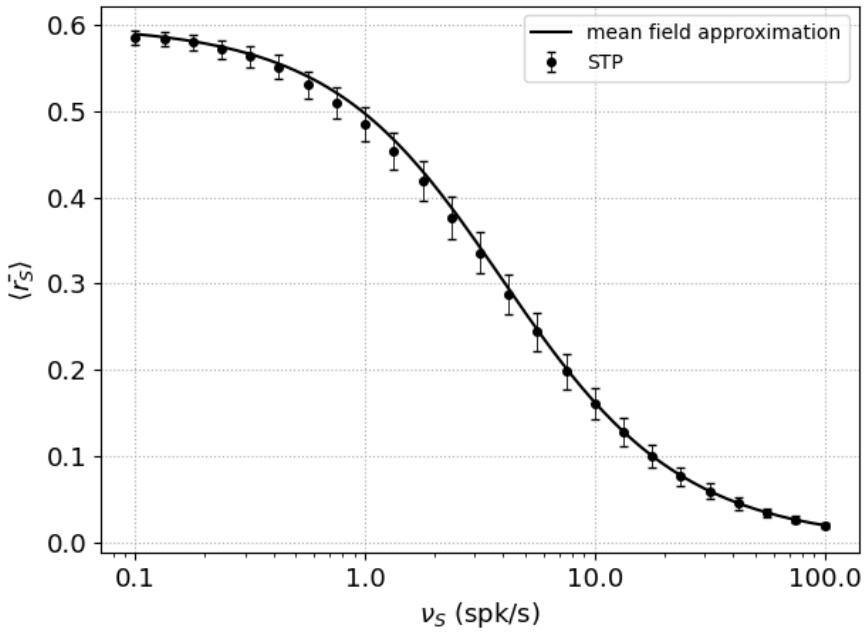

Figure 3.1: **Average release probability for TM model and mean field approximation solution**. Mean field approximation (3.7) and simulated data of r_S. Mean field approximation satisfying fit numerical data: $\chi^2 = 0.91$. Mean and standard error are computed over 30 different runs with the same initial condition for all ν_S values. Time simulation cover 500 second, only data after 334 second are taken to evaluate mean and standard error. Integration steps of 1 ms. Parameters as in table in Appendix B.1

Both numerical data and approximation solution help to give import insight about synaptic release in the presence of short-term plasticity. When presynaptic firing rate is low than facilitation and depression time constant, i.e. $\nu_S \ll \Omega_f$, Ω_d, synaptic variables reach their initial values and, as a consequence, the dynamics is equal to the total absence of plasticity. On the other hand, intense presynaptic firing rate provides strong depletion of resources that drastically reduce neurotransmitter exocytosis and, as a consequence,

the synaptic strength.

Despite its apparent simplicity, The TM model can generate surprisingly complex dynamics due to the presence of the combination of facilitation and depression. With the mathematical background of mean field derivation, we can investigate the nature of a TM synapse and in particular the nature of transitions between facilitating and depressing responses. The slope of (3.8) with respect to input frequency ν_S can be used to distinguish between facilitating and depressing synapse. Indeed, a negative slope implies that the increment of r_S decreases regarding the input frequencies, hence the occurrence of depression, otherwise a positive slope reflects ongoing facilitation. Notably, for the limit of small input frequency, the slope is equal to

$$\langle \bar{r_S} \rangle' (\nu_S \to 0) = \frac{\Omega_d - (\Omega_d + \Omega_f) u_0}{(\Omega_f \Omega_d)^2} \tag{3.9}$$

which can be either positive or negative depending on the sign of the numerator, therefore the threshold value of basal release probability reads as

$$u_\theta = \frac{\Omega_d}{\Omega_d + \Omega_f} \tag{3.10}$$

Depending on whether u_0 is respectively below or above the threshold value u_θ, the synaptic transmission switch from depressing to facilitation and vice versa: the depressing synapse is defined by the condiction $u_0 > u_\theta$, facilitating one by $u_0 < u_\theta$. That is the crucial point because the gliomodulation add degrees of freedom on parameters u_0, thus we can appreciate a transition between the two regime mode of synaptic transmission due to astrocytic activity.

3.2 Tripartite Synapses

In line with the description of gliomodulation introduced in section 2.3, the tripartite synapses could be seen as a three compartmental model: (i) bipartite synapse with short-term plasticity (3.1), (ii) astrocytic calcium-dependent gliotransmitter and (iii) neurotransmitters and gliotransmitter time course in the extracellular space (ECS). For the sake of clarity, we reported here equations of G-ChI model

$$\begin{aligned}
\frac{d\Gamma_A}{dt} &= O_N Y_S (1 - \Gamma_A) - \Omega_N \left(1 + \zeta \mathcal{H}_1(C, K_{KC})\right) \Gamma_A \\
\frac{dC}{dt} &= J_r(C.h, I) + J_l(C) - J_p(C) \\
\frac{dh}{dt} &= \frac{h_\infty(C, I) - h}{\tau_h(C, I)} \\
\frac{dI}{dt} &= J_\beta(\Gamma_A) + J_\delta(C, I) - J_{3K}(C, I) - J_{5P}(I),
\end{aligned} \tag{3.11}$$

and the time course of chemicals in ECS:

$$\begin{aligned}
\frac{dY_S}{dt} &= -\Omega_c Y_S + \sum_k Y_{rel} \delta(t - t_k) \\
\frac{dG_A}{dt} &= -\Omega_e G_A + \sum_j G_{rel} \delta(t - t_j)
\end{aligned} \tag{3.12}$$

The synaptic modulation can be presented in two different situations relating to the interaction pathway among these elements. Indeed, gliotransmitter exocytosis could be modulated both by the very synapses that are regulated by the astrocyte, in the so-called *homosynaptic* scenario of gliotransmission (equations (3.11)) and by synapses that are not, consistently with a *heterosynaptic* scenario. The latter kind of connection where the astrocytic activity is considered independent of the synaptic one is used to describe how the gliotransmitter could change the synapse's short-term plasticity in the simplest situation. Then, the extension to the more realistic closed-loop is straightforward taking to account the additional term of astrocytic activity dependence on the extracellular space. At this early stage, we want to stress that one of the peculiar aspects of neuron-glia interaction is the diverse time scale of neuronal (of the order of milliseconds) and glial (tons of seconds) dynamics. This difference will play a paramount role both in the microscopic and mesoscopic description.

3.2.1 Heterosynaptic Connection - open loop

In heterosynaptic connection, the onset of Ca^{2+} oscillations depends only on endogenous IP_3 production which rewords into the absence of the J_β flow in equation (3.11). The one-directional pathway makes only the astrocyte influences the synaptic dynamics, thus it is quite undemanding to analyse how the presynaptic release probability r_S is modulated by release-decreasing gliotransmission. All the effects regardings release-decreasing gliotransmission are found in the dynamics of basal release probability described in equation (2.21), the limit case happens when α is equal to 0, thus the time course of u_0 becomes

$$u_0(t) = (1 - \Gamma_S(t))U_0^* \tag{3.13}$$

In the simple bipartite scenario, the presynaptic receptors are totally silent due to the absence of gliotransmitters in ESC hence the model falls back to a short-term plasticity one with $u_0 = U_0^*$. Otherwise, at a GRE a cert amount of gliotransmitter are released and detected by presynaptic receptors. Therefore Γ_S, according to the first ODE in (3.11), grows exponentially at the rate $O_G G_A$ and then decreases in the same trend at the rate Ω_G. The increasing mechanism leads to the decreasing of u_0 which is generally lower than in the simple synapses, from this the name release-decreasing effect, whereas the exponential inactivated process of receptors provides an increase of basal release probability during two consecutive GREs. Figure (3.2) illustrates the above considerations and, in particular, we can merely appreciate modulation effects for time observation in the order of several seconds.

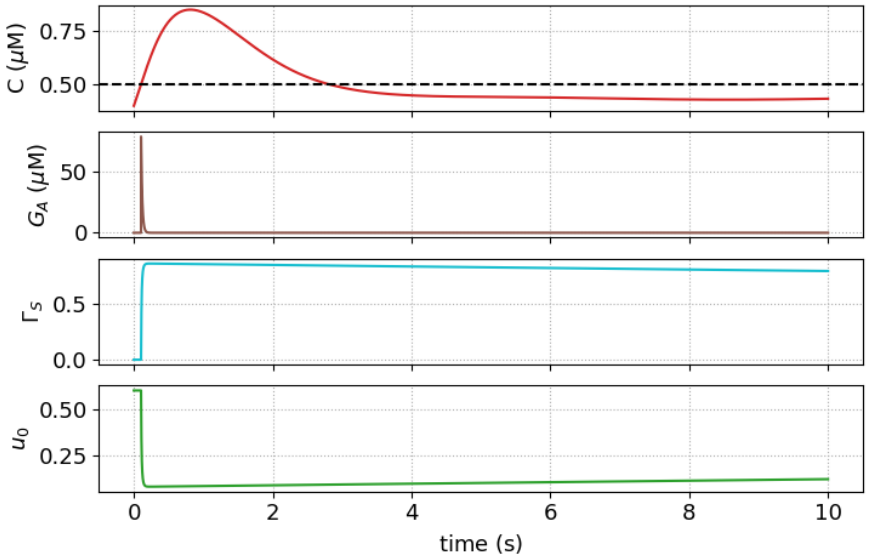

Figure 3.2: **Modulation of basal released probability on open-loop scenario.** Astrocytic calcium oscillation in open-loop scenario (red trace) drives the release of gliotransmitter in ESP (brown trace). Gliotrasmitter release at time 97.55 ms triggers an increase of Γ_S, (light blue trace) with the notable effects in the decreasing of basal release probability u_0. According to the characteristic time scale, the modulation effects are visible for observation time in the order of several seconds. Time simulation of 10 seconds with integration step of 0.05 ms.

Notably, these considerations arising from the heterosynaptic connection are completely general and might be present also in the more realistic homosynaptic connection. The core is the activation and inactivation processes of the presynaptic receptor regardless of the selected model. Indeed, the meaningful result of the astrocytic activity is the extension of the phase space, the basal release probability is not further a constant but is a dynamical variable of the model. The natural question is how this new degree of freedom changes the synaptic transmission.

Remarkably, contrary to common sense, the release-decreasing effect does not provide only the drop of neurotransmitter's exocytosis, but also the gliotransmitter-induced facilitation effect. We have already reported the facilitation effect in bipartite synapses in section 2.2 where it is the mechanism by which the concentration of released neurotransmitters increases with the incoming action potentials. We might appreciate a facilitation event in correspondence to an increase of available resources that could ensue when the lag between the $(i-1)$-th and i-th action potentials is smaller than the lag between the i-th and $(i+1)$-th ones, that stands for the scenario of *recovery from depression* (RFD). The degree of freedom related to u_0 makes possible, for transient time observation, the effect of facilitation even if the inter-spikes interval between consecutive action potentials does not satisfy the above condition. Moreover, it is not out of sense to suppose that this transient time is proportional to the intensity of the astro-neuron connection. One of the parameters that regulates the interaction's strength is the gliotransmitter concentration released at each exocytosis, indeed an increase of G_T leads to an increase of G_A and the activation of a greater fraction of presynaptic receptors, therefore the basal release probability is strongly modulated (top panel in Figure (3.3)). The aforementioned effects can be quantified by considering synaptic release due to pairs of spikes, and computing for

each pair the paired-pulse ratio (PPR) of the fraction of neurotransmitter released by the first one

$$\mathrm{PPR} = \frac{r_{S_{i+1}}}{r_{S_i}}. \tag{3.14}$$

When PPR < 1 the neurotransmitter released by the second AP is less than the amount released by the first AP (depression effect), conversely, if PPR > 1 the synaptic release increases with the incoming action potential (facilitation effect).

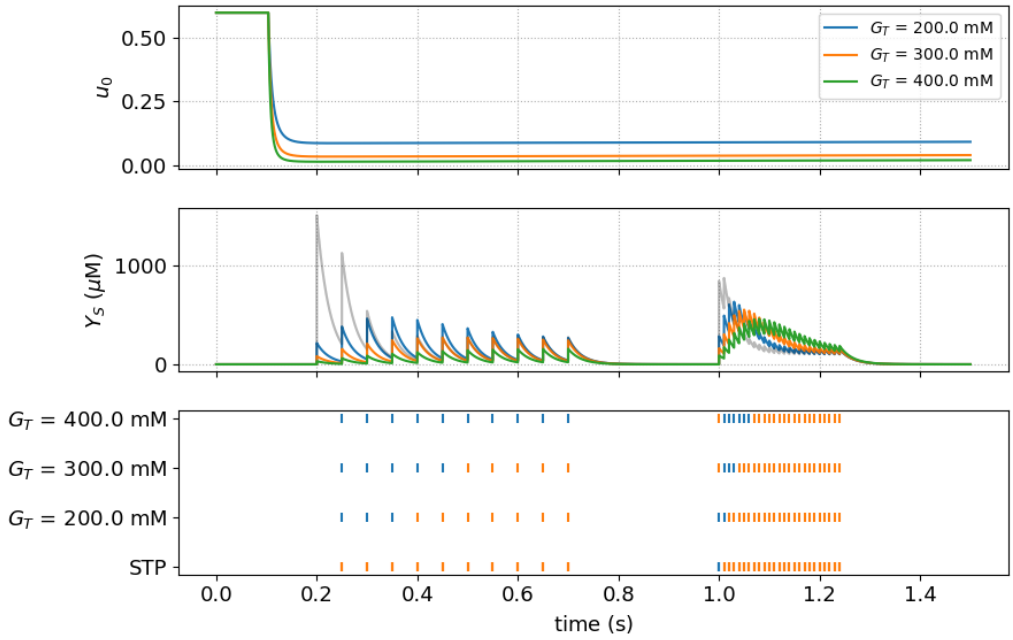

Figure 3.3: **Gliotransmitter-induced facilitation with respect to G_T in open-loop circuit.** STP and gliotransmitter-induced facilitation effect. Presynaptic firing rate is composed of two distinct regions, the former with 20 spk/s and the latter 100 spk/s. (Top panel) Increasing the gliotransmitter release leads to an increase of Γ_S, as a consequence the basal release probability falls to 0. (Middle panel) Neurotransmitter released by consecutive action potentials shows different behaviour that can be quantified by the PPR factor. (Bottom panel) Every release event is coloured in orange (depression) and blue (facilitation), the transient time of facilitation effect changes across the strength of gliotransmission. Time simulation of 1.5 seconds with integration step of 0.05 ms.

The bottom panel in Figure (3.3) summarized the most peculiar results that can be appreciated. In the case of simple STP and with weak gliomodulation, the depletion events dominate the facilitation ones however, in the latter scenario the glio-induced facilitation is present as well as the RFD. The transient time of facilitation is further extended with strong gliomodulation moreover the RFD event is not more visible. In conclusion, the combination of depletion and facilitation drives the synaptic transmission that changes in heterosynaptic connection. Without gliotransmission, the extracellular neurotransmitter concentration progressively decreases, whereas this amount tends to increase at every action potential whit respect to the preceding one in presence of gliomodulation (middle panel in Figure (3.3)).

Mean field description of Gliotrasmission modulation

A mean field description of gliorelease events could be found following the same procedure of neurotransmitter release, noting that a release event by an astrocyte is described by the

same model of synaptic release in 3.1. With this aim, the first important observation is that nucleation of spontaneous spikes in astrocytes, namely in the open-loop circuit, may be approximated by a Poisson process with time-dependent frequency $\nu_A(t)$. Importantly, the exact expression of the GRE rate is not crucial for the validity of mean-field derivation, what is crucial is the Poisson assumption. The mean field equivalent of equations (2.17) and (2.18) reads as

$$\begin{aligned}\frac{d\langle \bar{x_A}\rangle}{dt} &= \Omega_A(1-\langle \bar{x_A}\rangle) - U_A\langle \bar{x_A}\rangle\nu_A(t)\\ \frac{d\langle \bar{G_A}\rangle}{dt} &= -\Omega_e\langle \bar{G_A}\rangle + \rho_e G_T U_A\langle \bar{x_A}\rangle\nu_A(t)\end{aligned} \tag{3.15}$$

in particular, experimental data suggest that the timescale of gliotransmitter modulation is much slower than the time course of the gliotransmitter in the ECS. Accordingly, it may be assumed that $\Omega_G \ll \Omega_A, \Omega_e$, and only the timescale slower than $1/\Omega_e$ can be considered in second equations (3.15) so that

$$\langle \bar{G_A}\rangle \approx \frac{\rho_e G_T}{\Omega_e} U_A\langle \bar{x_A}\rangle\nu_A(t) \tag{3.16}$$

substituting the above equation in (2.22), and averaging the latter, provides

$$\begin{aligned}\frac{d\langle \bar{\Gamma_S}\rangle}{dt} &= J_S U_A\langle \bar{x_A}\rangle(1-\langle \bar{\Gamma_S}\rangle)\nu_A(t) - \Omega_G\langle \bar{\Gamma_S}\rangle\\ J_S &= \rho_e\frac{O_G G_T}{\Omega_e}\end{aligned} \tag{3.17}$$

the above equations can generally be used to reliably estimate the mean field dynamics of basal release probability

$$\langle \bar{u_0}\rangle = U_0^* + (\alpha - U_0^*)\langle \bar{\Gamma_S}\rangle \tag{3.18}$$

Finally the equations (3.15), (3.17) and (3.18) provide a mean field description of gliorelease event and the modulation of basal release probability by astrocyte. For constant astrocytic firing rate, i.e. $\nu_A(t) = \nu_A$ is relevant considering the steady state solution of $\langle \bar{x_A}\rangle$, $\langle \bar{\Gamma_S}\rangle$ and $\langle \bar{u_0}\rangle$.

$$\begin{aligned}\langle \bar{x_A}\rangle &= \frac{\Omega_A}{\Omega_A + U_A\nu_A}\\ \langle \bar{\Gamma_S}\rangle &= \frac{J_S\Omega_A U_A\nu_A}{\Omega_A\Omega_G + (J_S\Omega_A + \Omega_G)U_A\nu_A}\end{aligned} \tag{3.19}$$

For a low astrocytic firing rate, $\nu_A \to 0$, the gliotransmitter resources tends to 1 and the fraction of presynaptic receptors tends to 0, thus the neurotransmitter modulation by astrocyte does not modify the basal release probability. For higher $\nu_A \to +\infty$, instead, x_A tends to 0 while Γ_S approaches to its limit value $J_S\Omega_A/J_S\Omega_A + \Omega_G$, in this situation the modulation is stronger than anything else and the basal probability tends to 0. Figure (3.4) shows the behavior of basal release probability for release-decreasing effect, in particular $\langle \bar{u_0}\rangle$ decreases with increasing ν_A

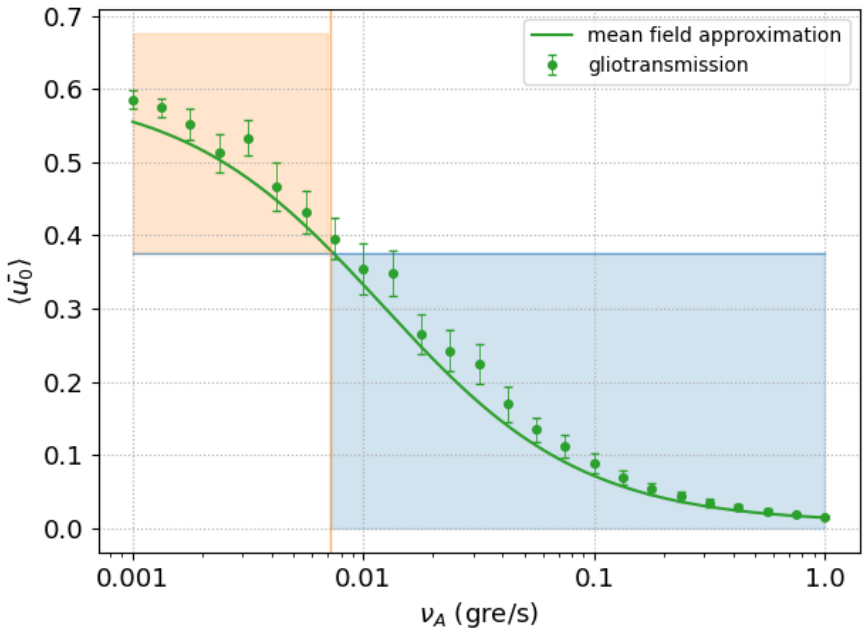

Figure 3.4: **Average basal release probability for heterosynaptic connection and mean field approximation solution**. Basal synaptic release probability is controlled by the rate of gliotransmitter release. For release-decreasing effect u_0 decrease with ν_A (green trance and dots) and a threshold ν_θ (orange vertical line) can be identified in correspondence of u_θ (horizontal blue line). The astrocytic firing rate drives the shift between depressing (orange-shaded region) and facilitating synapses (blue-shaded region). Mean field approximation (3.19) and simulated data of u_0. Mean field approximation solution satisfying fit numerical data: $\chi^2 = 1.80$. Time simulation cover 1200 second, only data after 800 second are taken to evaluate mean and standard error. Integration steps of 1 ms. Parameters: $\Omega_G = 0.08$ Hz and $O_G = 0.5\ \mu\mathrm{M}^{-1}\mathrm{s}^{-1}$.

The curve $\langle \bar{u_0} \rangle$ versus ν_A also shows that for a particular value of the GRE rate, denoted by ν_θ (vertical orange line), basal release probability crosses the threshold release probability u_θ (horizontal blue line). Such frequency ν_θ can be regarded as the threshold rate of gliotransmitter exocytosis that makes a synapse switch its mode of transmission and plasticity. That is, a depressing synapse, that is originally characterized by $u_0 > u_\theta$, could turn facilitating for $\nu_A > \nu_\theta$ in the presence of release-decreasing gliotransmission whereby $u_0 < u_\theta$ (Figure (3.4), blue-shaded area).

3.2.2 Homosynaptic Connection - closed loop

In the previous discussion, we have only considered one-way interactions between synapse and astrocyte, the modulation of synaptic release by gliotransmission. However, in the general case, the other possible pathway namely the astrocytic activity dependence on synaptic release may coexist with the other in the closed-loop circuit. Indeed, the synaptic exocytosis triggers in astrocytes an addiction mechanism of IP_3 production depending on extracellular neurotransmitters concentration. The exogenous IP_3 production profoundly affects the dynamics of I and, for the strong nonlinear coupling with C, also the onset of calcium oscillation and the timing of gliorelease events as reported in Figure (3.5).

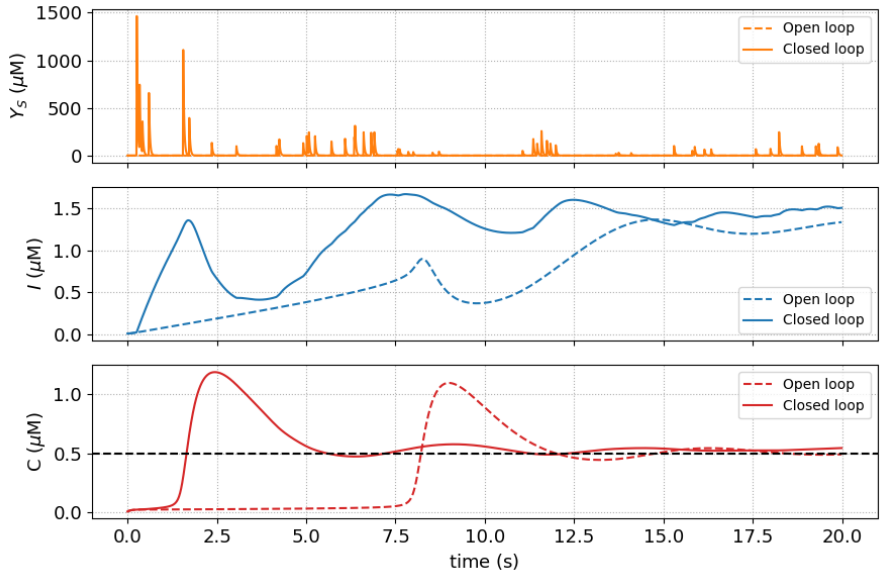

Figure 3.5: **Differences between astrocyte dynamics in open- and close- loop**. Astrocytic variable dynamics in open- (dashed) and closed-loop (solid) circuit. Exogenous IP_3 production deeply changes the I time evolution and this is reflected in the onset of calcium oscillations. Time simulation and integration steps are respectively equal to 20.0 seconds and 0.05 ms, the initial conditions are equals in both open- and closed- loop scenario.

In the brain, the motley types of connection provide that a single neuron receives a cert amount of synaptic inputs from a pool of presynaptic neurons which may or may not form connections with astrocytes. In this sense, the average across several synaptic release events in the bipartite and tripartite synapses sheds light on the functional implications of gliotransmission. Figure 3.6 shows the time evolution of average neurotransmitter concentration in the synaptic cleft in response to a constant input rate. Gliotrasmission dramatically changes synaptic transmission: after a gliorelease event, the neurotransmitters abruptly decrease both in open- and closed loops, and then increase according to the facilitation effect tenting to reach the concentration in the simple situation. The notable differences are found in GRE distribution shown in the right panel, the astrocytes in heterosynaptic connection are independent of synaptic activity, hence fire at the same time whereas in closed-loop the bidirectional coupling makes the distribution of GREs sparser. Despite the timing of exocytosis events by astrocytes, the inactivation and activation process of presynaptic receptors are the main protagonists in tripartite synapses. More precisely, the rate of the inactivation process can be interpreted as the drift moving the systems toward its baseline condiction, namely without gliomodulation, hence an increase

in Ω_G gets the presence of astrocytic activity less weighty and the synaptic transmission tends to be equal to bipartite synapses one (Figure (3.7) A). Similarly, the activation process regulates the susceptibility of the synapse to the concentration of gliotransmission, thereby increasing O_G leads to faster release-decreasing effects (Figure (3.7) B).

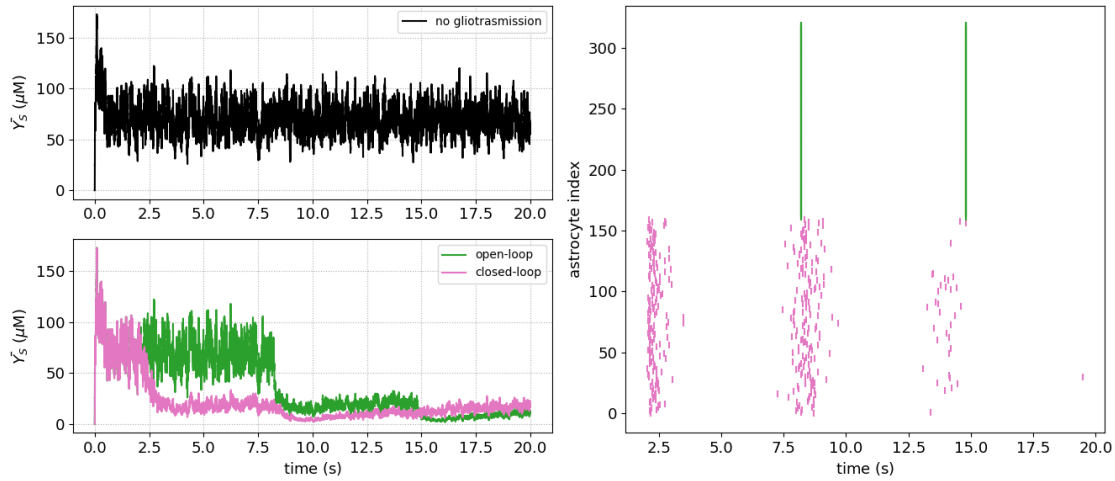

Figure 3.6: **Average neurotransmitter release in case of bipartite and tripartite synapses**. Average neurotransmitter release across 160 independent and identical synapses for 20 second long simulation with identical initial condiction. The presynaptic firing rate is generated by the homogeneous Poisson process with $\nu_S = 3.5$ (spk/s). In simple synapses (black trace) $\bar{Y_S}$ have a constant mean value of 70 $\pm$ 15 μM over all time simulation, gliotransmission modulation of u_0 deeply changes this dynamical behaviour both in open- (green trace) and closed-loop (pink trace). Raster plot of GRE, astrocytes labeled from 0 to 160 (pink marker) are part of closed-loop, the other one (green) of open-loop. Initial conditions: I=C=0.01 μM, h=0, Y_S=0 μM. Time simulation cover 20 second with integration steps of 0.05 ms.

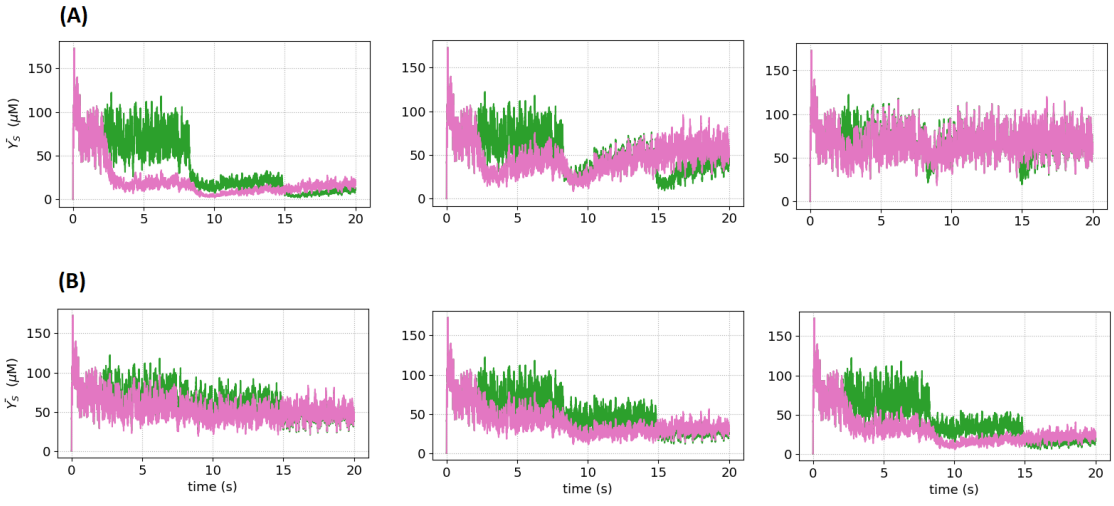

Figure 3.7: **Depressing and Facilitation effects with respect to Ω_G and O_G.**. Inactivation and activation of presynaptic receptor drive respectively facilitation (A) and depression (B) effects. Time simulation cover 20 second with integration steps of 0.05 ms. Parameters: (A) $O_G = 1.5$ μM^{-1}s^{-1}, from left to right $\Omega_G = 0.0083$ s^{-1}, $\Omega_G = 0.0833$ s^{-1}, $\Omega_G = 0.8333$ s^{-1}. (B) (B) $\Omega_G = 0.0083$ s^{-1}, from left to right $O_G = 0.3$ μM^{-1}s^{-1}, $O_G = 0.6$ μM^{-1}s^{-1}, $O_G = 0.9$ μM^{-1}s^{-1}

Filtering characteristic

The differences in terms of signalling transmission between bipartite and tripartite synapses are further elucidated by looking at the average synaptic release for different rates of randomly incoming action potentials. In this way, we may analyse the nature of filtering behaviour in presence of gliotransmitters release. We have already depictured in Figure (3.1) how short-term plasticity in bipartite synapses affects neurotransmitter release as a low-pass filter. Indeed, for the selected facilitation and depression rate, r_S exponentially decreases for increasing inputs rate, hence only low frequencies can carry out the signal to the target neurons. Moreover, the gliomodulation induced by heterosynaptic connection allows the synapses to dynamically switch their transmission mode through the value of gliorelease rate. Nevertheless, the astrocytic exocytosis happens when intracellular calcium concentration overreaches a threshold value, furthermore, the neuron-astrocyte interaction became much more intricate in homosynaptic connection. Indeed, the bidirectional coupling makes the inner astrocytic dynamics dependent on the synaptic one, in other words, the modulation of gliorelease by synaptic is beside the modulation of synaptic release by the glia. It is pleonastic to underline that a quantitative description of such complex systems is far more demanding than the previous ones, however, we have enough information, also through the numerical effort, to deduce a qualitative description of synaptic transmission in the closed-loop scenario.

Firstly, the calcium oscillations across the threshold are mandatory to observe the gliomodulation and their temporal scale drives the depletion and facilitation effects. Additionally, in the closed-loop the type of connection makes the dynamics of the whole system totally regulated by the presynaptic spikes train, namely ν_S is regarded as control parameter. The bifurcation plots are suitable tools to individuate the range of control parameter for which the gliomodulation is present.

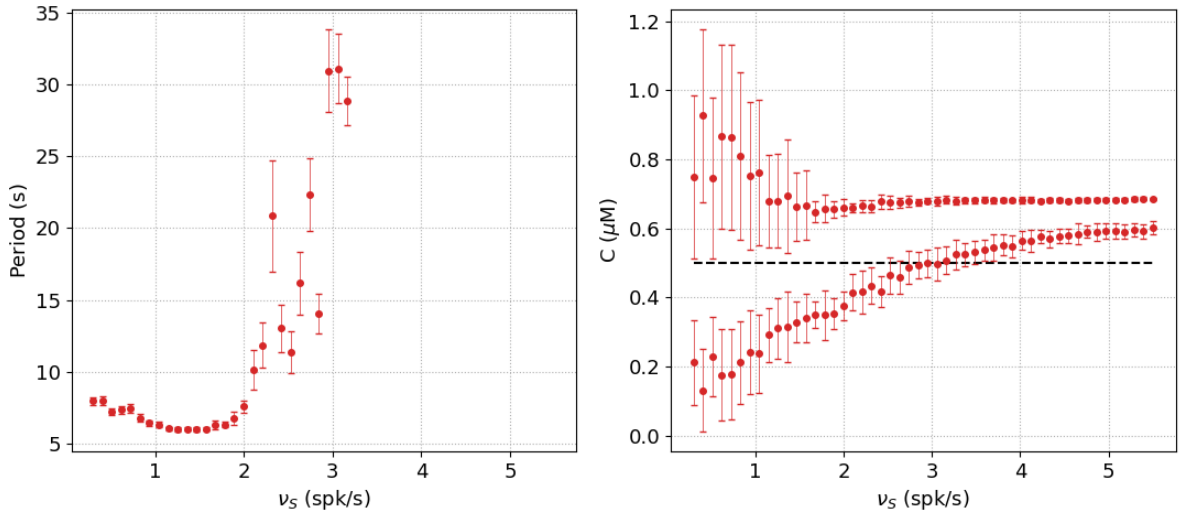

Figure 3.8: **Bifurcation analyses of noisily closed-loop synapses**. Calcium oscillations across the threshold arise for low presynaptic firing rate (right panel) with increasing periods (left panel). Mean and standard error are computed over 30 different runs with the same initial condition for all ν_S values. Time simulation cover 500 second, only data after 400 second are taken to compute bifurcation plots. Integration steps of 0.05 ms. Parameters: $O_\beta = 2.0\ \mu\text{Ms}^{-1}$, $O_\delta = 0.6\ \mu\text{Ms}^{-1}$, $O_G = 1.5\ \mu\text{M}^{-1}\text{s}^{-1}$, $\Omega_G = 0.0083\ \text{s}^{-1}$

As illustrated in the right plot of Figure (3.8), the oscillations across the threshold are visible for low inputs rate whereas they are above the threshold for ν_S greater than $\sim$ 3 spk/s. The periods of such oscillations also show an increasing dependence on the presynaptic firing rate. This particular behaviour gives us an important clue about the modulation of basal release probability. The modulation of astrocytic activity by synaptic release provides a relation between gliotransmitters and neurotransmitters release rate, i.e. $\nu_A \equiv \nu_A(\nu_S)$ as reported in the left panel of Figure (3.8). More precisely, the inversely proportional relation leads to null astrocytic firing rates in correspondence with high input rates. Thus, we expect the modulation of u_0 and the switch between transmission modes to be regulated by ν_S which is an emergent behaviour not present in naive synapses where the signalling modality depends exclusively on facilitation and depression parameters. Indeed, we can appreciate the switch from facilitating to depressing mode with increasing presynaptic firing rate (Figure(3.9)).

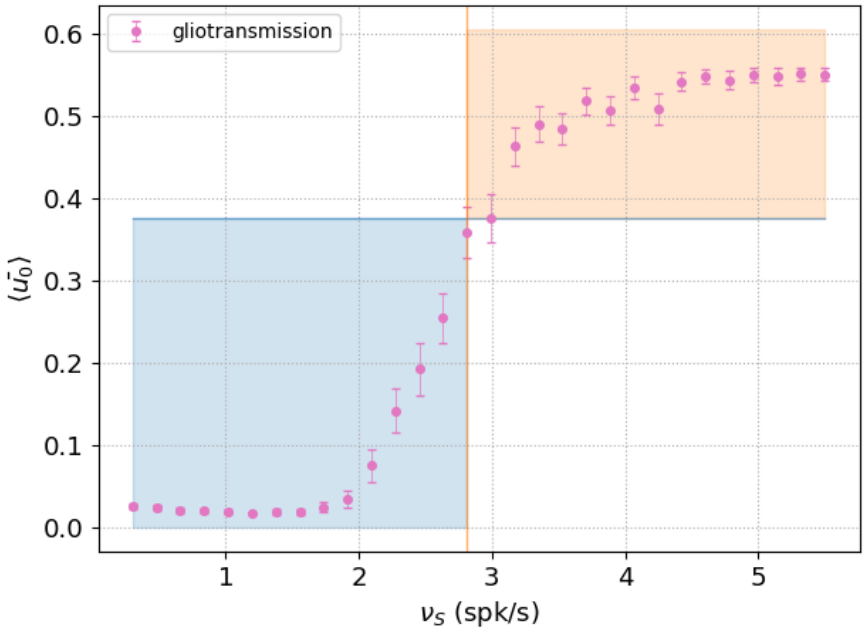

Figure 3.9: **Average basal release probability for homosynaptic connection**. The mean value of u_0 in the closed-loop (pink dots) scenario shows a symmetric behaviour with respect to open-loop one. Presynaptic firing rate regulates the transition mode from facilitating (blue-shaded region) for low ν_S to depressing synapses (orange-shaded region). Mean and standard error are computed over 20 different runs with the same initial condition for all ν_S values. Time simulation cover 500 second, only data after 334 second are taken to evaluate mean and standard error. Integration steps of 0.05 ms. Parameters: $O_\beta = 2.0\ \mu\text{Ms}^{-1}$, $O_\delta = 0.6\ \mu\text{Ms}^{-1}$, $O_G = 1.5\ \mu\text{M}^{-1}\text{s}^{-1}$, $\Omega_G = 0.0083\ \text{s}^{-1}$

In the facilitation region (blue-shaded region), the release probability increases with consecutive action potentials at a rate defined by the inactivation mechanism of the presynaptic receptor (Ω_G). With a wide temporal scale of these deactivation process, i.e. on the order of minutes, and in correspondence with intense gliotransmitters exocytosis, the value of u_0 is constantly modulated by release decreasing effect at rate $O_G G_A$. The lower astrocytic activity ensues in the neighbourhood of cert threshold value ν_θ (orange vertical line) which able the system to tend at its baseline condition that comes only in the total absence of glial activity, namely in the depression region (orange-shaded region). This condition occurs when the concentration of neurotransmitters in the cleft is so elevated

that does not allow the deactivation process of the astrocytic membrane receptor needed for the onset of gliorelease.

All the ensuing features from the above qualitative description are condensate in the filtering feature. Only low input rates could modulate neurotransmitter release probability and make the synapse more silent than in the absence of an astrocyte whereas, high input rates cannot further sustain gliotransmitter release and the release probability equals the case of simple synapses. This is elucidated in Figure (3.10) where the filter characteristic of simple bipartite synapse is compared with tripartite synapses in closed-loop one. The low-pass filter characteristic of synapses without gliotransmission (black dots) turns into a bell-shaped, band-pass filter characteristic caused by homosynaptic connection (pink dots).

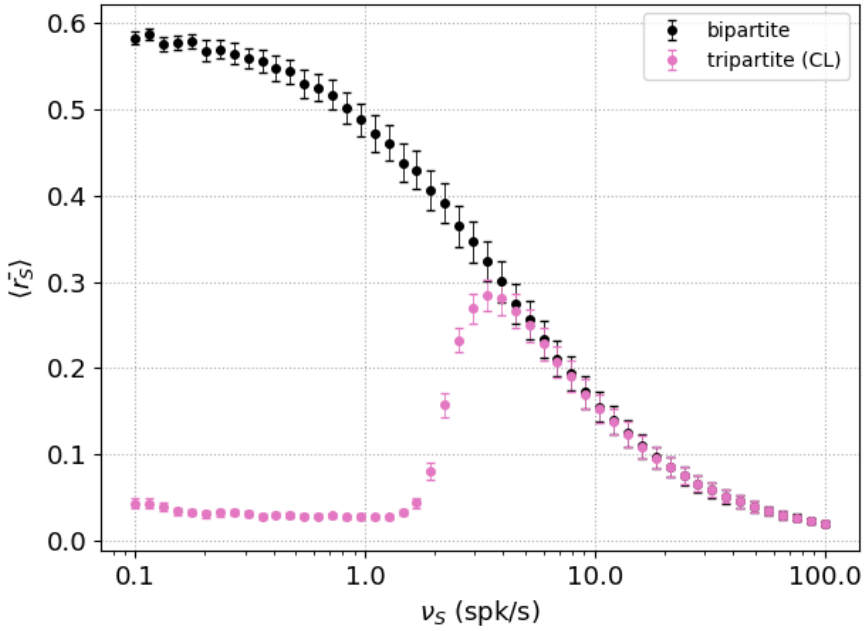

Figure 3.10: **Average release probability for TM model of bipartite synapses and closed-loop tripartite synapse ones.** Filtering characteristic curve passes from low-pass filter for bipartite synapse to a band-pass filter for tripartite one. . Mean and standard error are computed over 30 different runs with the same initial condition for all ν_S values. Time simulation cover 500 second, only data after 334 second are taken to evaluate mean and standard error. Integration steps of 1 ms. Parameters: $O_\beta = 2.0$ μMs^{-1}, $O_\delta = 0.6$ μMs^{-1}, $O_G = 1.5$ $\mu\text{M}^{-1}\text{s}^{-1}$, $\Omega_G = 0.0083$ s^{-1}

According to the above considerations, the emergent aspect induced by glia is the possibility to process the external input in two distinct ways and this occurs in a dynamical fashion depending on the frequency of the input. Indeed, the modulation of synaptic filtering by gliotransmission offers the possibility that the same stimulus could be differently processed and transmitted to the postsynaptic target in the presence or not of surrounding astrocytic processes, ultimately providing synapses with a versatile processing feature with respect to incoming action potential.

3.2.3 Mean field description of homosynaptic connection

The mean field derivations of neurotransmitters release probability in simple short-term plasticity synapses in section 3.1 and of the gliotransmission modulation in section 3.2.2

are the starting points of a possible analytical description of homosynaptic connection. The fundamental assumptions used to deduce the steady states of mean-dynamical variables are the statistical independence and the description by Poisson processes of neurotransmitters and gliotransmitters release, moreover, by definition, the basal release probability in heterosynaptic connection is independent of synaptic dynamics. Therefore, the sets of relations (3.7) and (3.19) describe the mean quantities of two totally disjointed systems. The great issue induced by homosynaptic connection is the link between these two systems that makes u_0 dependent on the very synaptic dynamics. Following the same kind of reasoning, we can deduce a mean field derivation of homosynaptic connection with the assumption of statistical independence between u_0 and u_S, accordingly the mean field dynamics reads as

$$\begin{aligned}
\frac{d\langle \bar{u_S}\rangle}{dt} &= \Omega_f(u_0 + \langle \bar{u_S}\rangle) + \langle \bar{u_0}\rangle(1 - \langle \bar{u_S}\rangle)\,\nu_S \\
\frac{d\langle \bar{x_S}\rangle}{dt} &= \Omega_d(1 - \langle \bar{x_S}\rangle) - \langle \bar{u_S}\rangle\langle \bar{x_S}\rangle\,\nu_S \\
\frac{d\langle \bar{x_A}\rangle}{dt} &= \Omega_A(1 - \langle \bar{x_A}\rangle) - U_A\langle \bar{x_A}\rangle\nu_A \\
\frac{d\langle \bar{\Gamma}_S\rangle}{dt} &= J_S U_A\langle \bar{x_A}\rangle(1 - \langle \bar{\Gamma}_S\rangle)\nu_A - \Omega_G\langle \bar{\Gamma}_S\rangle \\
\langle \bar{u_0}\rangle &= U_0^* + (\alpha - U_0^*)\langle \bar{\Gamma}_S\rangle
\end{aligned} \tag{3.20}$$

The information about the bidirectional coupling is embedded into the relation between ν_A and ν_S. Therefore, assuming the presynaptic firing rate as a control parameter, we need to deduce a cert biological function $\nu_A \equiv \nu_A(\nu_S)$, thus the equations (3.20) become

$$\begin{aligned}
\frac{d\langle \bar{u_S}\rangle}{dt} &= \Omega_f(u_0 + \langle \bar{u_S}\rangle) + \langle \bar{u_0}\rangle(1 - \langle \bar{u_S}\rangle)\,\nu_S \\
\frac{d\langle \bar{x_S}\rangle}{dt} &= \Omega_d(1 - \langle \bar{x_S}\rangle) - \langle \bar{u_S}\rangle\langle \bar{x_S}\rangle\,\nu_S \\
\frac{d\langle \bar{x_A}\rangle}{dt} &= \Omega_A(1 - \langle \bar{x_A}\rangle) - U_A\langle \bar{x_A}\rangle\nu_A(\nu_S) \\
\frac{d\langle \bar{\Gamma}_S\rangle}{dt} &= J_S U_A\langle \bar{x_A}\rangle(1 - \langle \bar{\Gamma}_S\rangle)\nu_A(\nu_S) - \Omega_G\langle \bar{\Gamma}_S\rangle \\
\langle \bar{u_0}\rangle &= U_0^* + (\alpha - U_0^*)\langle \bar{\Gamma}_S\rangle
\end{aligned} \tag{3.21}$$

Without experimental data, a possible procedure to find the guess function is the qualitative approach, more precisely analyses how the tripartite synapse responds to noiseless input. A constant external input leads to inter-spikes interval distribution having a delta function-like fashion, accordingly for each value of ν_S the probability release does not change with incoming action potential even in the presence of synaptic dynamical behaviour.

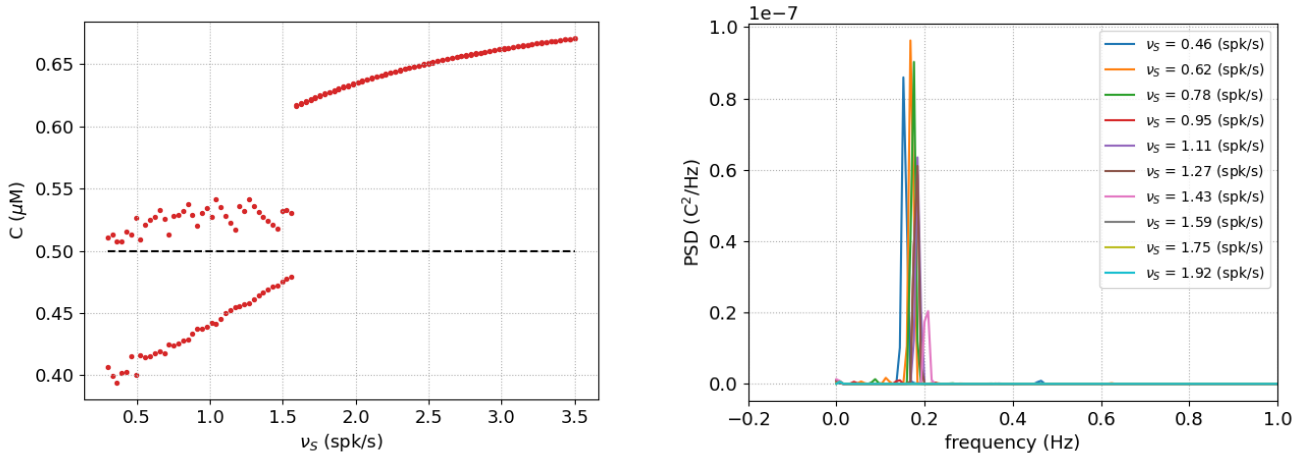

Figure 3.11: **Bifurcation plot and power spectral density of noiseless closed-loop synapses.** Noiseless bifurcation analysis (right plot) shows bifurcation for low frequencies input rate and different amplitude of calcium oscillation, power spectrum densities suggest the amplitude modulation [14]. Parameters: $O_\beta = 2.0\ \mu\text{Ms}^{-1}$, $O_\delta = 0.6\ \mu\text{Ms}^{-1}$, $O_G = 1.5\ \mu\text{M}^{-1}\text{s}^{-1}$, $\Omega_G = 0.0083\ \text{s}^{-1}$

With these aims, we can individuate the possible range of input signals for which the gliomodulation occurs. Indeed, as reported in the left panel of Figure (3.11), the oscillations across the threshold with varied amplitudes turn into suprathreshold steady states for $\nu_S = \nu_S^{bif}$. This qualitative change in dynamical features can be regarded as a bifurcation and used as a guide to deduce a guess function for $\nu_A(\nu_S)$. The power spectrum in the right panel of Figure (3.11) indicates the oscillations arise at constant frequencies, otherwise the steady states do not sustain any kind of gliomodulation. These evidences suggest for a guess function a step-like one, however, to consider a continuous relation between ν_A and ν_S we select an exponential decay with characteristic time τ_A to link the two regions. Finally, for $\nu_A(\nu_S)$ is proposed the following expression:

$$\nu_A = \begin{cases} \nu_A = \frac{1}{T_A} & \text{with } \nu_S < \nu_S^{bif} \\ \nu_A = \frac{1}{T_A} \exp -(\nu_S - \nu_S^{bif})\tau_A & \text{with } \nu_S > \nu_S^{bif} \end{cases} \tag{3.22}$$

Chapter 4

NEURON-GLIA NETWORKS: RESULTS

4.1 Neural Network and the effects of STP

4.2 Long-Term effect of gliomodulation

Appendix A

Mean field approximation

A.1 Validity of Mean Field Description

The statistical independence assumption of the variable in mean field derivation induces an error. This approximation error has been estimated for bipartite synapses and heterosynaptic scenarios by the Cauchy-Swarz inequality of probability theory in [18, 10]:

$$\frac{|\langle ab\rangle - \langle a\rangle\langle b\rangle|}{\langle a\rangle\langle b\rangle} \leq \mathrm{CV}_a\ \mathrm{CV}_b \tag{A.1}$$

a and b are two generic variables whereas CV_a and CV_b are the respectively coefficient of variation. Only if $\mathrm{CV}_a\,\mathrm{CV}_b < 0.1$ provides a realistic description o synaptic dynamics. In the derivation of the mean field description of homosynaptic connection, the independence between astrocyte and synapses is embedded in the independence of u_S and u_0. The coefficient of variation of u_0 with $\alpha = 0$ is obtained from the equation 3.13

$$\mathrm{CV}^2_{u_0} = \frac{\langle u_0^2\rangle - \langle u_0\rangle^2}{\langle u_0\rangle^2} = \frac{U_0^{*2}(\langle \Gamma_S^2\rangle - \langle \Gamma_S\rangle^2)}{(U_0^* - U_0^*\langle \Gamma_S\rangle)^2} = \mathrm{CV}^2_{\Gamma_S}\frac{\langle \Gamma_S\rangle^2}{(1-\langle \Gamma_S\rangle)^2} \tag{A.2}$$

The self-consistency of the mean field derivation can now be checked by plotting the product of CV_{u_S} and CV_{u_0}

$$\begin{aligned} \mathrm{CV}^2_{u_S} &= \frac{\Omega_f(1-\langle u_0\rangle)^2\nu_S}{(\Omega_f+\nu_s)(2\Omega_f + \langle u_0\rangle(2-\langle u_0\rangle)\nu_S} \\ \mathrm{CV}^2_{u_0} &= \frac{\langle \Gamma_S\rangle^2}{(1-\langle \Gamma_S\rangle)^2}\frac{\Omega_G^2}{(_G+(1-\beta)\nu_A)(\Omega_G+(1+\beta)\nu_A)} \end{aligned} \tag{A.3}$$

where $\beta = \exp -J_S U_A$. In section 3.2.2 we have elucidated ha the activation and deactivation process of presynaptic receptors regulate the modulation of u_0, accordingly these mechanisms handle the validity of statistical independence. Indeed, the reactivity of Γ_S dynamics for high values of the rates $_G$ and Ω_G leads to the coefficient of variation exceeding the 10% in the neighbour of $\nu_S = 1.0$ spk/s as reported in Figure (A.1)

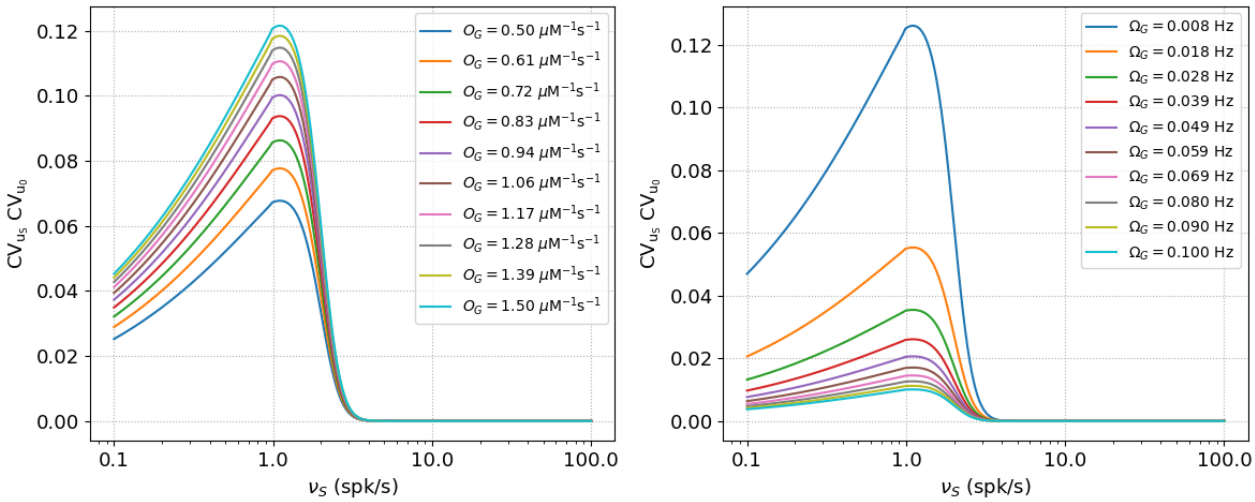

Figure A.1: **Validation of mean field approximation for homosynaptic scenario**. Validation of statistical independence with respect to O_G (left panel) and Ω_G (right panel) Parameters: (left panel) $\Omega_G = 0.0083\ s^{-1}$, $O_\beta = 3.2\ \mu Ms^{-1}$, $O_\delta = 0.6\ \mu Ms^{-1}$; (right panel) $O_G = 1.5\ \mu M^{-1}s^{-1}$, $O_\beta = 3.2\ \mu Ms^{-1}$, $O_\delta = 0.6\ \mu Ms^{-1}$

A.2 χ^2 Test

For the analysis in figure (3.1), the numerical estimations of r_S for different values of incoming spikes trains ν_S are compared with mean field analytical approximations. For each value of ν_{S_i}, we have obtained a sample of r_{S_i} distributed with a cert probability distribution around its mean. The quantity used to quantify the agreement between the analytical solution and the data is the reduced chi squared χ^2_r:

$$\chi^2_r = \frac{1}{N_s} \sum_i^{N_S} \frac{(\langle r_S \rangle_i - \langle r_S \rangle_{i-st})^2}{\sigma^2_{\langle r_S \rangle_i}} \tag{A.4}$$

where N_S is the total number of data and $\langle r_S \rangle_{i-st}$ the analytical estimation. The χ^2 satisfies a well precise probability distribution when the data are independent and normally distributed. A value of χ^2_r close to 1 suggests that the approximation solutions differ from numerical data as well as the data differs among the trials, thus a value of the reduced chi squared means a good fit between model and data.

Appendix B

Parameters

Values of parameters used in the simulation are summarized the following tables. Parameters values are taken from previous published studies [12].

For istance, d_i for $i = 1, 2, 3, 5$ comes reduction method that leads to Li Rinzel model from De Young-Keizer one, for detailed derivation see [7]. Astrocytic parameters are taken from [14, 12].

B.1 Neurons ans Synapses

Symbol	Name in code	Value	Units	Description
			Neuron parameters	
C_m	`C_m`	198	pF	Membrane capacitance
E_i	`E_i`	-60	mV	Leak reversal potential
g_l	`g_l`	9.99	nS	Leak conductance
V_r	`V_r`	-60	mV	Reset potential
V_θ	`V_th`	-50	mV	Firing threshold
τ_r	`tau_r`	5	ms	Refractory period
			Synapses parameters	
Ω_d	`Omega_d`	2	s^{-1}	Synaptic depression rate
Ω_f	`Omega_f`	3.33	s^{-1}	Synaptic facilitation rate
U_0	`U_0`	0.6	-	Resting synaptic release probability
w_e	`w_e`	50	pS	Excitatory synaptic conductance
w_i	`w_i`	1	nS	Inhibitory synaptic conductance
τ_e	`tau_e`	5	ms	Excitatory synaptic time constant
τ_i	`tau_i`	10	ms	Inhibitory synaptic time constant
E_e	`E_e`	0	mV	Excitatory synaptic reversal potential
E_i	`E_i`	-80	mV	Inhibitory synaptic reversal potential
			Presynaptic receptors	
O_G	`O_G`	1.5	$\mu M^{-1}s^{-1}$	Activation rate per mole
Ω_G	`Omega_G`	0.5	min^{-1}	Synaptic facilitation rate

B.2 Astrocyte

Symbol	Name in code	Value	Units	Description
		Ca^{2+}-induced Ca^{2+} release		
C_T	C_T	2	μM	Total cell free Ca^{2+} content
ρ_A	rho_A	0.18	-	ER-to-cytoplasm volume ratio
d_1	d_1	0.13	μM	IP_3 binding affinity
d_2	d_2	1.05	μM	Ca^{2+} inactivation dissociation constant
d_3	d_3	0.9434	μM	IP_3 dissociation constant
d_5	d_5	0.08	μM	Ca^{2+} activation dissociation constant
O_2	O_2	0.2	μM s^{-1}	IP_3R binding rate for Ca^{2+} inhibition
Ω_C	Omega_C	6	s^{-1}	Maximal rate of Ca^{2+} release by IP_3Rs
Ω_L	Omega_L	0.1	s^{-1}	Maximal rate of Ca^{2+} leak from the ER
O_P	O_P	0.9	μM s^{-1}	Maximal Ca^{2+} uptake rate by SERCAs
K_P	K_P	0.05	μM	Ca^{2+} affinity of SERCAs
		IP_3 signaling		
O_β	O_beta	0.5	μM s^{-1}	Maximal rate of IP_3 production by PLCβ
O_δ	O_delta	1.2	μM s^{-1}	Maximal rate of IP_3 production by PLCδ
κ_δ	kapppa_delta	1.5	μM	Inhibition constant of PLCδ by IP_3
K_δ	K_delta	0.1	μM	Ca^{2+} affinity of PLCδ
O_{3K}	O_3K	4.5	μM s^{-1}	Maximum rate of IP_3 degradation by IP_3-3K
K_{3K}	K_3K	1.0	μM	IP_3 affinity of IP_3-3K
K_D	K_D	0.7	μM	Ca^{2+} affinity of IP_3-3K
Ω_{5P}	Omega_5P	0.05	s^{-1}	Maximal rate of IP_3 degradation by IP-5P
		Metabotrobic receptor kinetics		
O_G	O_N	0.3	μM s^{-1}	Agonist binding rate
Ω_G	Omega_N	0.5	s^{-1}	Maximal inactivation rate
K_{KC}	K_KC	0.5	μM	Ca^{2+} affinity of PKC
ζ	zeta	10	-	Maximal reduction of receptor affinity by PKC
		Gliotrasmission		
C_θ	C_theta	0.5	μM	Ca^{2+} threshold for exocytosis
G_T	G_T	200	mM	Total vesicular Gliotransmitter concentration
Ω_A	Omega_A	0.6	s^{-1}	Gliotransmitter recycling rate
U_A	U_A	0.6	-	Gliotransmitter release probability
ρ_e	rho_e	6.5 10^{-4}	-	Astrocitic vesicle-to-extracellular volume ratio
Ω_e	Omega_e	60	s^{-1}	Gliotransmitter clearence rate
α	alpha	0	-	Gliotrasmission nature

Bibliography

[1] Verkhratsky A., Butt A. *Glial Neurobiology. A Textbook*, John Wiley Sons Ltd, 1rs eds. (2007)

Arthur Butt

[2] De Pittà M. Neuron-Glial Interactions, in: Jaeger D., Jung R. (eds) *Encyclopedia of Computational Neuroscience*. Springer, New York, NY. (2020)

[3] Somjen GG. Nervenkitt: notes on the history of the concept of neuroglia. Glia. 1(1):2-9. (1988)

[4] Virchow R. *Die Cellularpathologie in ihrer Begründung auf physiologische und pathologische Gewebelehre*. Berlin: August Hirschwald (1858).

[5] Perea G. et al. Neuron-glia networks: integral gear of brain function, *Frontiers in Cellular Neuroscience*, vol. 8. (2014)

[6] De Pittà M., Berry H. A Neuron-Glia Perspective for Computational Neuroscience. In: De Pittà, M., Berry, H. (eds) *Computational Glioscience*. Springer Series in Computational Neuroscience. Springer, Cham. (2019)

[7] Timofeeva J., Intracellular Calcium Dynamics: Biophysical and Simplified Models. In: De Pittà, M., Berry, H. (eds) *Computational Glioscience*. Springer Series in Computational Neuroscience. Springer, Cham. (2019)

[8] De Pittà, M., Ben-Jacob, E., Berry, H. G Protein-Coupled Receptor-Mediated Calcium Signaling in Astrocytes. In: De Pittà, M., Berry, H. (eds) *Computational Glioscience*. Springer Series in Computational Neuroscience. Springer, Cham. (2019)

[9] Lallouette J. et al. Astrocyte Networks and Intercellular Calcium Propagation. In: De Pittà, M., Berry, H. (eds) *Computational Glioscience*. Springer Series in Computational Neuroscience. Springer, Cham. (2019)

[10] De Pittà M., Gliotransmitter Exocytosis and Its Consequences on Synaptic Transmission. In: De Pittà, M., Berry, H. (eds) *Computational Glioscience*. Springer Series in Computational Neuroscience. Springer, Cham. (2019)

[11] Stimberg M., et al. Modeling Neuron–Glia Interactions with the Brian 2 Simulator. In: De Pittà, M., Berry, H. (eds) *Computational Glioscience*. Springer Series in Computational Neuroscience. Springer, Cham. (2019)

[12] De Pittà M., Brunel N. Modulation of Synaptic Plasticity by glutammatergic Gliotransmission: A Modeling Study, *Neural Plasticity*, vol. 2016, Article ID 7607924, 30 pages, (2016).

[13] De Pittà M, Volman V, Levine H, Pioggia G, De Rossi D, Ben-Jacob E. Coexistence of amplitude and frequency modulations in intracellular calcium dynamics. *Phys Rev E Stat Nonlin Soft Matter Phys.* 77(3 Pt 1) (2008)

[14] De Pittà M., Goldberg, M., Volman, V. et al. Glutammate Regulation of Calcium and IP3 Oscillating and Pulsating Dynamics in Astrocytes. *J Biol Phys* 35, 383–411 (2009).

[15] De Pittà M., Volman V., Berry H., Ben-Jacob E. A tale of two stories: astrocyte regulation of synaptic depression and facilitation. *PLoS Comput Biol.* 7(12). (2011)

[16] Gerstner W et al. Theory and Simulation in Neuroscience. *Science*, vol. 338, n. 6103, pp. 60-65. (2012)

[17] Tsodyks M.V., Markram H. The neural code between neocortical pyramidal neurons depends on neurotransmitter release probability. *Proc Natl Acad Sci USA*, 94:719–723, (1997)

[18] Tsodyks M, Pawelzik K, Markram H. Neural networks with dynamic synapses. *Neural Comput.* 10(4):821-35. (1998)

[19] Tsodyks M.V. Activity-dependent transmission in neocortical synapses. In: Chow C, Gutkin B, Hansel D, Meunier C, Dalibard, J (eds) *Methods and models in neurophysics* (Chap. 7). Elsevier, pp 245–265. (2005)

[20] Brunel, N. Dynamics of Sparsely Connected Networks of Excitatory and Inhibitory Spiking Neurons. *J Comput Neurosci* 8, 183–208 (2000).

[21] Brunel N, Wang XJ. What determines the frequency of fast network oscillations with irregular neural discharges? I. Synaptic dynamics and excitation-inhibition balance. *J Comput Neurosci.*90(1):415-30. (2001)

[22] Mazzoni A, Panzeri S, Logothetis NK, Brunel N. Encoding of naturalistic stimuli by local field potential spectra in networks of excitatory and inhibitory neurons. *PLoS Comput Biol.* 4(12):e1000239. (2008)

[23] Cressman, J.R., Ullah, G., Ziburkus, J. et al. The influence of sodium and potassium dynamics on excitability, seizures, and the stability of persistent states: I. Single neuron dynamics. *J Comput Neurosci.* 26, 159–170 (2009).

[24] Ullah, G., Cressman Jr., J.R., Barreto, E. et al. The influence of sodium and potassium dynamics on excitability, seizures, and the stability of persistent states: II. Network and glial dynamics. *J Comput Neurosci* 26, 171–183 (2009).

[25] Savtchenko Leonid P. and Rusakov Dmitri A. Regulation of rhythm genesis by volume-limited, astroglia-like signals in neural networks. *Phil. Trans. R. Soc. B* 369 20130614. 20130614. (2014)

[26] Poincaré H.J. Sur le problème des trois corps et les équations de la dynamique. *Acta Mathematica*, vol. 13, pp. 1-270 (1890)

[27] Strogatz S.H. *Nonlinear Dynamics and Chaos. With Application to Physics, Biology, Chemistry, and Engineering* . CRC Press, 2nd eds, (2015).

[28] Wiggins S. *Introduction to Applied Nonlinear Dynamical Systems and Chaos*. Springer, 2nd eds, (2003)

[29] Meiss J.D. *Differential Dynamical Systems*. SIAM. (2008)

[30] Izhikevich E. M. *Dynamical Systems in Neuroscience: The Geometry of Excitability and Bursting*. The MIT Press Cambridge, (2010)

[31] Sterratt, D., Graham, B., Gillies, A., Willshaw, D. *Principles of Computational Modelling in Neuroscience*. Cambridge: Cambridge University Press. (2011)

[32] Ermentrout G.B., Terman D.H. *Mathematical Foundations of Neuroscience*. Springer, Interdisciplinary Applied Mathematics vol. 35. (2010)

[33] Gerstner W., Kistler W., Naud R., Paninski L. *Neuronal Dynamics: From Single Neurons to Networks and Models of Cognition*. Cambridge: Cambridge University Press, (2014)

[34] Hodgkin A.L, Huxley A.F. A quantitative description of membrane current and its application to conduction and excitation in nerve. *The Journal of physiology*, 117(4), 500–544. (1952)

[35] Hodgkin A.L. The local electric changes associated with repetitive action in a non-medullated axon. *The Journal of Physiology*, 107(2), 165–181. (1948)

[36] Izhikevich E.M., FitzHugh R. FitzHugh-Nagumo model. *Scholarpedia*, 1(9):1349. (2006)

[37] Morris C., Lecar H. Voltage oscillations in the barnacle giant muscle fiber. *Biophysical Journal*, Vol. 35, Issue 1, pp. 193-213 (1981)

[38] Burkitt A.N. A review of the integrate-and-fire neuron model: I. Homogeneous synaptic input. *Biol Cybern*. 95(1):1-19. (2006)

[39] Faisal A.A., Selen L.P.J., Wolpert D. M. Noise in the nervous system. *Nature Reviews Neuroscience*, 9(4), 292–303. (2008).

[40] Softky W., Koch C. The highly irregular firing pattern of cortical cells is inconsistent with temporal integration of random EPSPs. *J Neurosci* 13:334–350 (1993)

[41] Skupin A., Falcke M. Statistical analysis of calcium oscillations. *Eur Phys J SpecTop* 187:231– 240 (2010)

[42] Keizer J, De Young GW. Two roles of Ca2+ in agonist stimulated Ca2+ oscillations. *Biophys J.61* (3):649-660. (1992)

[43] Li YX, Rinzel J. Equations for InsP3 receptor-mediated [Ca2+]i oscillations derived from a detailed kinetic model: a Hodgkin-Huxley like formalism. *J Theor Biol*. 166(4):461-73. (1994)

[44] Tsodyks M.V., Markram H. The neural code between neocortical pyramidal neurons depends on neurotransmitter release probability. *Proc Natl Acad Sci* U S A. 94(2):719-23. (1997)

[45] Michaelis L, Menten ML, et. al. The original Michaelis constant: translation of the 1913 Michaelis-Menten paper. *Biochemistry.* 4;50(39):8264-9. (2011)

[46] Araque A, Parpura V, Sanzgiri RP, Haydon PG. Glutamate-dependent astrocyte modulation of synaptic transmission between cultured hippocampal neurons. *Eur J Neurosci.* 10(6):2129-42. (1998a)

[47] McKenna T.M., McMullen T.A., Shlesinger M.F. The brain as a dynamic physical system. *Neuroscience.* 60(3):587-605. (1994)

[48] Richmond B.J. Information Coding. In: *Encyclopedia of Neuroscience*, 137–144 (2009)

[49] Destexhe A., Bedard C. Local Field Potential *Scholarpedia*, 8(8):10713. (2013)

[50] Bushong A. et al. Protoplasmic Astrocytes in CA1 Stratum Radiatum Occupy Separate Anatomical Domains, *Society for Neuroscience*, vol. 22, n. 1, pp. 183-192, (2002)

[51] Cannelli A. *Metodologie sperimentali in Fisica* third eds, EdiSES. (2010)